Flight and scaling of flyers in nature

U.M. Lindhe Norberg
Department of Zoology, University of Göteborg, Sweden.

Abstract

Flight is one of the most demanding adaptations found in nature because of the physical problems in remaining airborne. Therefore, fliers in nature have been subjected to strong selection for optimal morphology. Different flight modes are associated with distinct wing design, dictated by the animal's niche and habitat selection. This paper focuses on vertebrate fliers. A main problem for flying animals and aircraft is to obtain enough lift in slow flight. Flapping flight always includes phases with unsteady flow, and in this situation the flexible animal wing has superior performance than a fixed aeroplane wing. Animals can manoeuvre better and change wing form to meet different flight conditions and requirements and they can also make compensating wing movements to avoid stall. Flying vertebrates have evolved several sophisticated lift-enhancing wing adaptations similar to those developed for flying machines, such as slots, slats, flaps and turbulence generators of the boundary layer. Dimensional analysis is a valuable tool in studies of the biomechanics and energetics of animal flight. Empirical allometric relationships allow exploration of how different mechanical, physiological and ecological constraints change in importance with size and wing form. Flight parameters, such as wing loading (weight/wing area) and aspect ratio (wingspan^2/wing area), are widely used both in aircraft engineering and in studies of animal flight. But the shape of the tail is also important; the tails of birds vary more than their wings. Regression of wing morphology and aerodynamic characteristics are also given for various vertebrate fliers, with a few comparisons with aircraft.

1 Introduction

Animal flight includes *gliding*, or passive flight without wingstrokes, and active, *flapping*, flight. Powered flight is an efficient way to transport a unit of body mass over a unit of distance. The cost of transport is lower than for running but more expensive than for swimming [1], but it is accompanied by a high rate of energy requirement per unit time. Flight also allows an animal to cross water and deserts, and to reach foraging sites inaccessible to many non-fliers. Flying animals have undergone a dramatic adaptive radiation because of such obvious advantages of flight.

Insects comprise the most diverse and numerous animal class with about 750,000 recorded species, and their size range spans from about 1 μg to about 20 g. Bats include about 1,000 species and weigh about 1.5 g to 1.5 kg, whereas birds include more than 8,800 species and weigh

WIT Transactions on State of the Art in Science and Engineering, Vol 3, © 2006 WIT Press
www.witpress.com, ISSN 1755-8336 (on-line)
doi:10.2495/1-84564-001-2/2d

about 1.5 g to 15 kg. Pterosaurs may have weighed from 4 g to 75 kg. *Quetzalcoatlus northropii*, the largest pterosaur found, had a wingspan of about 11 m. The largest extinct bird (*Argentavis magnificens*) may have weighed 80–100 kg and had a wingspan of about 3.5 m. Its high wing loading would have been ill-suited for flight under poor thermal conditions, but useful in slope-soaring on uprising air current against hillsides [2].

Much of our understanding of flight mechanics in animals is based on analogy with aircraft. In steady level flight, an aircraft as well as a flying animal must generate lift force to support weight against gravity and propulsive thrust against drag. While aircraft produce thrust with an engine, animals have to flap their wings. This means that in a flapping animal every flight parameter (wing area, wingspan, angle of attack, etc.) changes during the wingstroke and along the wing, and the flow around the wings can be very unsteady. This makes flight force and power calculations much more complicated for animals than for fixed-wing aircraft. Furthermore, flexible wings require particular adaptations in the muscular and skeletal systems in order to maintain strength and high performance. However, a main benefit of flapping wings compared with fixed-wing aircraft is that animals can manoeuvre better and have a better possibility to change wing form in different flight situations. They can also make compensating wing movements to get out of stall. Bats and birds systematically twist their wings to change the angle of attack and corresponding lift. In this way they receive different amounts of lift on the two wings and can perform rolling and other manoeuvres. They can also move their tails for lift production and flight manoeuvres.

Flying animals are adapted to different niches, which means that they are using particular flight modes, which in turn are associated with different wing morphology. Some hover, some hawk insects in the air, while others fly continuously during foraging and still others forage in trees, bushes or on the ground, all of which requiring particular adaptations for high flight performance and low costs [3, 4]. However, often, there are conflicting selection pressures for high flight performance, so the optimal morphology can sometimes be difficult to interpret. For example, one particular wing form may be optimal for a bird species during the breeding season, but would contribute to expensive flight during migration. Furthermore, we often find sexually evolved ornaments among animals, such as long tails in birds, which often provide extra costs during flight [5, 6]. Thus, we find a large variety of combinations of morphological, ecological and behavioural attributes of flying animals. But the present combination of traits is usually assumed to represent a near-optimal solution, maximizing the fitness of the individual. Wake patterns depend on both flight morphology and speed and can be predicted for various flight gaits. The flight kinematics and vortex patterns of a flying animal are described in other chapters of this book, so these are only briefly mentioned here. This paper will not describe aerodynamic theories thoroughly; it will only discuss some basic aerodynamics for various flight modes as well as scaling of flight based on empirical data. The wing and tail design in birds and bats are also discussed.

There is a range of methods for the determination of flight forces and power for aircraft as well as animals. They can be estimated adequately by the lifting-line model associated with vortex formation, which was already formulated nearly hundred years ago (1910) in the Prandtl–Zhuhovsky–Lanchester vortex explanation [7]. Already in the 1930s and 1940s a number of interesting papers relating to the dynamics of flapping flight of birds appeared. Tikhonravov [8] expounded the vortex theory for flapping wings and pointed out the significance of the viscosity of air. Golubev [9, 10] described the thrust mechanism of flapping wings and Brown [11, 12] the wingbeat kinematics in pigeons. Gladkov [13] explained problems concerned with soaring in birds, and described wingbeat kinematics and devices for eliminating unsteadiness. Soaring flight was further studied by Vinogradov [14] and in more detailed by Cone [15, 16].

Pioneering works for the theoretical treatment of flight in insects, birds and bats include publications by Cone [17], Pennycuick [18–21], Tucker [22], Weis-Fogh [23, 24], Norberg

[25, 26], Rayner [27–29] and Ellington [30, 31], which have been of great importance and have formed the base for later studies on animal flight. Insect flight has been thoroughly studied by Brodsky, who summarized his own and others work in the comprehensive book *The Evolution of Insect Flight*' [32]. Theoretical models for animal flight are summarized in [33–41].

2 Dimensionless numbers that are important for flight dynamics

2.1 Lift and drag coefficients

The lift and drag coefficients for finite wings, C_L and C_D, are dimensionless parameters that indicate the capacity of an aerofoil to generate lift and drag at a given angle of attack. These coefficients are dependent on the shape of the aerofoil, the Reynolds number and the downwash angle, the latter depending on the wing's angle of attack.

There are only two basic mechanisms by which a force may be forwarded to a body moving through a flow, the *pressure* and *shear* distribution over the surface. The resultant force, F, integrated over the whole surface, is, by convention, decomposed into one drag component, D, normal to the direction of the freestream velocity, U, and one lift component, L, parallel to it. Lift and drag coefficients are functions of the lift and drag, respectively, and are expressed as

$$C_L = L/qS \quad \text{and} \quad C_D = D/qS, \tag{1}$$

where q is the dynamic pressure ($q = 0.5\rho U^2$, ρ being the air density) and S is the one-sided wing area (see Sections 3.1 and 3.2).

2.2 Reynolds number

The Reynolds number, Re, is the most important parameter affecting the lift and drag coefficients over the entire size range of aircraft and flying animals. It represents the ratio of inertial to viscous forces in a flow, $\mathrm{Re} = \rho U l/\mu$, where U is velocity, l is a characteristic length (such as wing chord) and μ is the viscosity of the flow. The ratio μ/ρ is the kinematic viscosity of the fluid. The flow pattern around a wing depends on this dimensionless number Re, which ranges from $\approx$1 (or even $<$1) for the smallest flying insects to $\approx 10^5 - 10^6$ for larger birds and bats, when it is defined at the mean wing chord. Greater kinematic viscosity (lower Re) means higher losses due to friction and reduced importance of inertia, whereas inertial forces are more important at higher Re.

Very near the wing surface the air is retarded due to friction, forming the boundary layer, which can be turbulent or laminar. The thickness of this layer decreases with increasing Re as long as the flow is laminar. When the boundary layer reaches a critical (minimum) thickness or some disturbance occurs, the laminarity gives way to turbulence. This can have both positive and negative effects (see Section 8.4).

Low and medium Reynolds number flight and flapping wing dynamics, characteristic of animal flight, involve detached flows and large-scale vortical motion. The Strouhal number then enters as a second important parameter for the dynamics.

2.3 Strouhal number

The Strouhal number is a dimensionless value that is useful for describing oscillating flow mechanisms and unsteady flow; it is a function of the Re number. The frequency f of a series of

eddies in a Kármán street behind a circular cylinder is proportional to the velocity of the incident flow U and inversely proportional to the diameter a of the circular cylinder [42]. In the formula $f = \mathrm{St}\, U/a$, at medium Reynolds numbers, the Strouhal number St ($= fa/U$) is a constant equal to 0.2. If an air current moving at $5\,\mathrm{m\,s^{-1}}$ impinges upon a wire that is 5 mm in diameter, eddies separate at a frequency $f = 0.2 \times 5/0.005 = 200\,\mathrm{Hz}$ [42].

The Strouhal number is bound to affect aerodynamic force coefficients and propulsive efficiency, probably by affecting the maximum aerodynamic angle of attack and the timescales of vortex growth and shedding [43–45]. Swimming and flying animals cruise at St values corresponding to a regime of vortex growth and shedding in which the propulsive efficiency of flapping foils peaks [45]. For flying animals f is taken to be the wingbeat frequency and a is amplitude, such as wingtip excursion. If St is too low (too low wingbeat frequency) then the resulting vorticity will be insufficient to provide a thrust component of the lift to overcome the drag on the wing.

Nudds *et al.* [46] showed that flying animals fly at an St number tuned for high power efficiency, and that St is a simple and accurate predictor of wingbeat frequency in birds. Typical values observed in nature for efficient swimming and flying are St = 0.2–0.4 [46].

The Strouhal number is related to the *reduced frequency* (the ratio between flapping velocity and forward speed at the half chord), which is the inverse of the *advance ratio* [31], both of which are often referred to in studies on animal flight. The reduced frequency is simply 2π times the corresponding St number.

3 Aerodynamic forces and power

Fluid motion is described by the Navier–Stokes equations, which comprise three, extremely complicated, equations describing each direction in a three-dimensional space. According to these equations the force available to accelerate a fluid particle is the vector sum of the pressure difference across it, its weight and the viscous force due to shear gradients in the surrounding fluid. Bernoulli's equation, generally adopted for studies of animal flight, is much simpler but it assumes that the flow is steady, that viscous forces are small enough to be ignored and that pressure losses are approximated by an empirical loss coefficient. However, appropriate simplifications provide models that make testable predictions. Using results from parametric tests, refinements of the model can be derived.

For simplicity, the equations for all forces are given as total forces for the whole wingstroke and wings (or animal), implying that these are the sums of forces at instantaneous positions and per unit span or area.

3.1 Lift and thrust

The production of lift and thrust is the crucial thing in the evolutionary pathway to powered flapping flight in animals. During flight wings with asymmetric profiles (in aircraft as well as in animals) force air to accelerate downwards, and the reaction towards the acceleration of air is the lift force. The wing surface forces passing air particles to change their momentary directions of motion. The initiated pressure changes then secondarily affect the local velocity along the motion line. Von Euler (1707–1783), mathematician and friend of Bernoulli, derived equations for how a fluid should behave around a body, assuming balance between local inertial and pressure forces. These equations were difficult to solve, but by assuming that the fluid was incompressible, Euler ended up with a relation that was similar to what Bernoulli had studied, which was why von Euler named it Bernoulli's theorem.

The pressure difference between the top and the bottom of the wing gives rise to a lift force, the magnitude of which depends on the freestream velocity U, the angle of incidence of the wing and the profile shape. The total lift experienced by the wings is given by the Kutta–Joukowski theorem as

$$L = \rho U b \Gamma, \tag{2}$$

where b is the wingspan. Circulation Γ is measured by the rate of rotation about the vortex lines, and can be expressed as a function of the lift coefficient, C_{L}, $\Gamma = (1/2)cVC_{\mathrm{L}}$, where c is the wing chord [47]. Since the wing area $S = bc$, lift can be expressed as

$$L = 0.5\rho U^2 S C_{\mathrm{L}}. \tag{3}$$

The magnitude of L (all forces given in newtons, $\mathrm{N} = \mathrm{kg\,m\,s^{-2}}$) thus varies with the size of the wing, the flight velocity and the lift coefficient. The coefficient can then be expressed as

$$C_{\mathrm{L}} = 2L\rho U^2 S, \tag{4}$$

where air density ρ is given in $\mathrm{kg\,m^{-3}}$, speed U in $\mathrm{m\,s^{-1}}$ and wing area S in $\mathrm{m^2}$.

Lift coefficients of 0.3–0.7 have been estimated with a steady, lifting surface analysis of a house sparrow in mid-downstroke [48]. The maximum lift coefficient, C_{Lmax}, for an ordinary non-permeable wing, obtained close to the stalling angle, is 1–2. Estimated C_{Lmax} in fruit bats is 1.5 [49] and 1.6 in a gliding hawk [50]. Wing slots (raised alula) can increase C_{Lmax} by about 10% [51, 52].

Weis-Fogh [23, 24], Pennycuick [49] and Norberg [25, 26] estimated an average coefficient of lift or L/D in birds and bats during flapping flight by using force equalization. The rationale behind their slightly different methods was to assume steady-state condition, then use quasi-steady-state aerodynamics, or blade-element analysis, and to contrast the results against the maximum lift coefficient, which may be 1.5–1.6. Values above this indicate unsteady conditions. The coefficients obtained in hovering bats and birds other than hummingbirds (using asymmetric hovering) are very high, indicating unsteady effects. Estimates of the mean downstroke lift coefficients in hovering animals vary between 1.1 for a bumblebee to 6 for a flycatcher (summarized in [40]).

In flapping flight aerodynamic forces are generated by actively moving wings. The velocity of the airflow meeting the wings in forward flight is the vector sum of the horizontal velocity, the velocity due to flapping and the velocity of the downwash (see below). The direction and magnitude of the resultant airflow will thus differ at each section of the chord along the wing length (Fig. 1) and during different phases of the wingstroke. Birds and bats are able to twist their wings to attain an optimal angle of attack along the entire wing. The degree of wing twisting required is related to flapping speed [52] and forward speed, which determine the direction of the relative air speed and thus the angle of incidence.

Thus, the total force experienced by the wings during the wingstroke is the sum of the forces on the different wing sections at the different stroke phases of the wingbeat cycle. The resultant force is conventionally divided into a vertical, upward, lift component and a horizontal positive thrust, T, or negative drag, D, component.

A dominant lift-generating mechanism in insect flight is the leading-edge vortices on their wings [53–55]. The sharp leading edges of insect wings induce high lift production through flow separation with vortical flow attached to the wing's upper surface. The arm wing of birds has a rounded leading edge, but that the edge of the hand wing is usually sharp. Videler *et al.* [56] applied digital particle image velocimetry using models of the wing of the common swift (*Apus apus*) in a water tunnel to investigate the lift generated by swept-back hand wings during gliding.

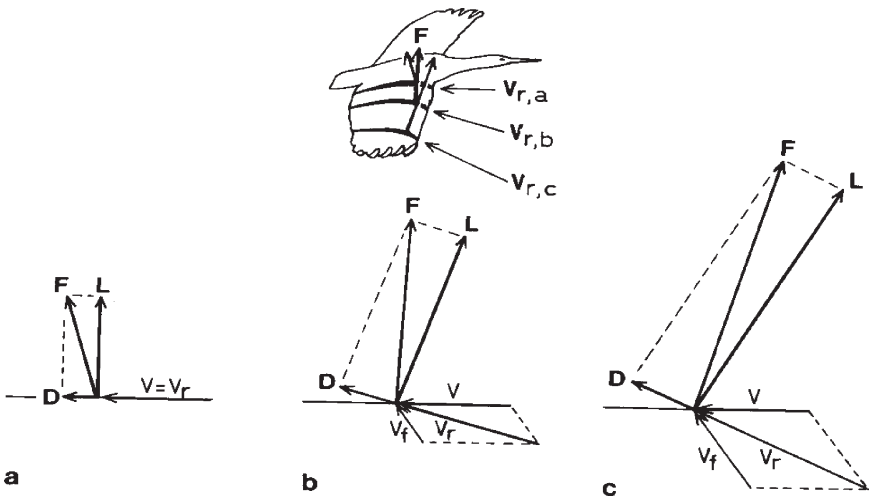

Figure 1: Force and velocity diagrams for the proximal part of the wing (a), the middle part (b) and the distal part (c) in a downstroke in horizontal flight. F is resultant force, L is lift force, D is drag force, V is forward velocity, V_f is flapping velocity and V_r is their resultant. From [34], courtesy of Springer-Verlag.

Their results showed that gliding swifts can generate stable leading-edge vortices at small angles (5°–10°) of attack and at Reynolds numbers as low as 3,750. The authors suggest that the flow around the arm wings of most birds can remain conventionally attached. Bats, on the other hand, have a sharp leading edge along the entire wing, which theoretically could generate leading-edge vortices during flight.

3.2 Drag forces

During flight the aerofoil also causes movements in the air flowing past and behind it. Air flowing downwards behind the wing provides a flow of momentum to give the upward lift force. At the Re numbers typical of flight in most birds and bats, this momentum of the air can only be transported as a vortex. These trailing vortices shed behind the wingtips are thus an inescapable consequence of force generation by the aerofoil.

Energy must be expended not only to generate these wake vortices but also to overcome form and friction drag on the wings and body. These energy losses are experienced as drag forces, D, which conventionally are set to act perpendicular to the lift force (see above). The energy invested in the vortices is experienced as *induced drag* (D_{ind}), and can be considerable in hovering and slow flight. The form and friction drag of the wings constitute the *profile drag* (D_{pro}) and that of the body is the *parasite drag* (D_{par}), both of which are large in fast flights.

The total drag coefficient can be expressed as

$$C_{\text{D}} = 2D\rho U^2 S. \tag{5}$$

Both lift and drag coefficients are often determined empirically. The average lift-to-drag ratio, L/D, of animal wings is usually less than 10, and it varies along the wing and during the wingstroke.

When a critical angle of attack (stalling angle) is exceeded, the airstream separates from the wing's upper surface with a sudden fall of C_{L} and increase of C_{D}. A good aerofoil maximizes the

pressure difference between its upper and lower sides and minimizes the drag (often maximizing L/D). An animal must either do mechanical work with its flight muscles to overcome drag or descend (glide or use partially powered flight) through the air at an angle where a component of its weight balances the drag. In steady level flight, lift L and weight mg, as well as thrust T and drag D, must be in equilibrium,

$$L = mg \quad \text{and} \quad T = D, \tag{6}$$

where m is the body mass (in kg) and g is the acceleration due to gravity (in $\mathrm{m\,s^{-2}}$).

The different drag components are related to different drag coefficients. The action of the wing with an arbitrary and continuous circulation (Γ) distribution can be analysed as a *lifting line* where the wake is composed of an infinite number of line vortices, and initially having the form of a vortex sheet shed at the trailing edge [29, 34, 40, 57]. The induced drag may then be calculated for any speed when the form of circulation distribution is given. The induced drag coefficient C_{Di} can be expressed as a function of the lift coefficient and the aspect ratio AR (wingspan/mean wing chord $= b^2/S$),

$$C_{\mathrm{Di}} = C_{\mathrm{L}}^2/e\pi\mathrm{AR}, \tag{7}$$

where $e \leq 1$ is the aerofoil efficiency factor. For an *elliptic* lift distribution $e = 1$, which gives the minimum loss of wingtip vortices for a given wing in steady motion. Thus, to reduce induced drag the wing should be long (high aspect ratio).

Whenever a three-dimensional flow occurs over the wing, the related *lifting surface* theory should be used instead, which includes that the induced downwash at any point in the surface is an integral of the vorticity (for a description, see [40]). Unsteadiness always occurs in flapping forward flight and depends on two things, the kinematics of the lifting surfaces and the time varying shedding of vorticity at separation points other than at the trailing edge, such as at the upper surface of the wings. The former can be measured by frequency parameters, which have been estimated and used to correct values obtained from quasi-steady aerodynamics. The latter can be detrimental and cause, for example, stall.

The average, effective, vortex-induced drag, derived from eqns (4) to (6), then is

$$D_{\mathrm{ind}} = 2k\,m^2g^2/\pi\rho b^2U^2, \tag{8}$$

where $k = 1/e$ and is a dimensionless 'induced drag factor' (>1) [34]. Experimental data suggest that $k \approx 1.1 - 1.2$[33]. The induced drag is important in hovering and slow flight, but decreases with increasing flight speed.

The profile drag includes two components, the friction drag, D_{f}, due to surface shear stress, and pressure or form drag, D_{p}, due to flow separation. Both are due to viscous effects. For an incompressible flow and a laminar boundary layer the coefficient of the friction drag is

$$C_{\mathrm{Df}} \approx k_0\mathrm{Re}^{-1/2}. \tag{9}$$

The proportionally constant k_0 is approximately 1.33 for a flat plate, but varies for different geometries. For turbulent boundary layers the friction drag coefficient is $C_{\mathrm{Df}} \approx \mathrm{Re}^{-1/5}$.

In the range $10^3 < \mathrm{Re} < 10^6$, where most bats and birds operate, the total drag coefficients are difficult to estimate. Both profile and parasite drag can be measured in wind tunnel tests, but empirical estimates of both are sensitive to changes in surface structure, angles of incidence and air turbulence. The profile drag depends on the profile drag coefficient, C_{Dpro}, and can be expressed as

$$D_{\mathrm{pro}} = 0.5SC_{\mathrm{Dpro}}U^2. \tag{10}$$

The drag of the body (parasite drag) is given by

$$D_{\text{par}} = 0.5 S_{\text{b}} C_{\text{Dpar}} U^2, \tag{11}$$

where S_{b} is the body frontal area and C_{Dpar} is its drag coefficient. The expression $S_{\text{b}}C_{\text{Dpar}}$ can be replaced by A_{e}, which is the area of a flat plate, transverse to the air stream, with $C_{\text{Dpar}} = 1$, which gives the same drag as the body ('equivalent flat plate area'; [21]). To minimize parasite drag the body should be streamlined, which is important for fast flying species since parasite drag increases with the square of the speed.

Experiments suggest that C_{Dpar} should be in the range 0.1–0.2 [58–60]. The area S_{b} was estimated in frozen birds (large waterfowl and raptor species) in wind tunnel measurements to be $S_{\text{b}} = 0.00813 m^{2/3}$ [61] Body (parasite) drag coefficients, measured in the same study, showed a tendency to be larger in small, slow birds (≈ 0.40) than in large, fast ones (≈ 0.25 for geese and swans), and intermediate for pigeon-sized birds. The relationship between body frontal area and mass among passerine birds was estimated to be $S_{\text{b}} = 0.0129 m^{0.61}$ [62].

Whereas vortex theory would be important for the calculation of the vortex-induced drag to give the most accurate estimates, quasi-steady theory is appropriate for the empirical formulation of the profile and parasite drag.

3.3 Flight power

3.3.1 Mechanical power

The flight muscles of the flying animal have to do mechanical work to support the body weight and overcome the form and friction drag of the body and the wings. The rate at which this work is done is the *mechanical* power required to fly (measured in watts, W), and is a function of speed,

$$P_{\text{mech}} = DU = mgU(D'/L'). \tag{12}$$

D'/L' is the inverse of the *effective* (average) lift-to-drag ratio, a dimensionless ratio referred to as the *cost of transport C* [21]

$$C = D'/L' = P_{\text{mech}}/mgU. \tag{13}$$

C represents the aerodynamic work done in transporting a unit body weight over a unit of distance, and is a valuable parameter in studies on bird migration.

Because the total drag is due to different things, the total mechanical power is the sum of different components. The *aerodynamic power* is the sum of the *induced*, *profile* and *parasite power*, corresponding to the induced, profile and parasite drag. A fourth component of the total power is the *inertial power*. It is the work needed to oscillate the wings, i.e. to accelerate and decelerate the mass of the wings during a wingbeat cycle, which decreases with decreasing wingspan and wing mass and increases with increasing flapping frequency. The inertial power is $P_{\text{iner}} = I\omega/t$, where I is the moment of inertia of the wings (which can be estimated by strip analysis), ω is the angular velocity of the wings and t is the wingstroke period [34].

The inertial power is often neglected because it is uncertain to what extent inertial power is converted into useful aerodynamic power [21, 23]. However, empirical data on wing lengths of birds with different flight behaviour indicate that inertial costs are important in hovering and slow-flying species [6]. If these costs do not exist or are minute, hovering and slow-flying birds should have long wings to reduce induced power. Mail birds displaying their tails in forward flight also benefit from elongated wings to compensate for increased parasite drag [63], but the short

wings of hovering birds, including the Jackson's widowbird (*Euplectes jacksoni*), suggest that inertial costs do exist and that they may be more important in hovering and slow flight than the induced power [6].

The total mechanical power required to fly can then be written as

$$\begin{aligned} P_{\text{mech}} &= P_{\text{ind}} + P_{\text{pro}} + P_{\text{par}} + P_{\text{iner}} \\ &= 2k(mg)^2/\rho U \pi b^2 + 0.5\rho U^3 S C_{\text{Dpro}} + 0.5\rho U^3 S_{\text{b}} C_{\text{Dpar}} + Iw/t. \end{aligned} \tag{14}$$

The induced power [the first term in eq (14)] is the rate at which work has to be done to form the wing wake. To reduce this component the weight should be low and the wingspan should be long, which is important particularly during slow flight. To reduce the wing profile power (second term) at a given flight speed, the wing area should be small, and to reduce the parasite power (third term) the body should be slim and streamlined. The induced power decreases with increasing flight speed, whereas the profile and parasite power components become increasingly important at higher speeds. Inertial power increases with wing length, wing mass and wingbeat frequency (see below).

3.3.2 Metabolic power

The rate at which fuel energy is required is the *metabolic* power, P_{met}. Muscles produce mechanical work from chemical energy, and most of this energy is then lost as heat. The mechanical power is $P_{\text{mech}} = \eta P_{\text{met}}$, where η is the mechanical efficiency value of the flight muscles giving the proportion of chemical energy converted into external work. In small flying birds and bats (weighing around 10 g) the mechanical efficiency can be as low as 0.10 or lower, whereas it can be 0.20–0.30 in larger birds. In addition there is a cost for resting (or basal) metabolism P_{b} and for circulation of the blood and ventilation of the lungs connected with flight activity. The metabolic power can therefore be written as $P_{\text{met}} = kP_{\text{mech}}/\eta + P_{\text{b}}$, where k is a circulation and ventilation factor, taken to be 1.10 [64].

3.3.3 Power curve

The theoretical mechanical power curve for the aerodynamic power (eqn (14) with the inertial power excluded) can be written in the form

$$P_{\text{mech}} = \alpha/U + \beta U^3, \tag{15}$$

where α and β are constants. This is the equation for a U-shaped curve, and its bottom point defines the *minimum power*, P_{mp}, and the *minimum power speed*, U_{mr}, at which the bird can fly the longest time on a given amount of energy [21] (Fig. 2). The tangent to the curve defines the *maximum range power*, P_{mr}, and the *maximum range speed*, U_{mr}, which should be used for maximization of flight distance on a given amount of energy [21]. The inertial power, which is required to accelerate the wing and the unknown virtual, 'added', mass of the fluid [cf. eqn (14)], is indicated by the shaded area in the diagram.

4 Gliding and soaring

In gliding flight the animal's flight muscles do not provide any power (other than to keep the wings outstretched and for correcting manoeuvres), which instead comes from the animal using up its potential energy. The costs for gliding flight during migration has been estimated to be approximately 3–4 times the basal metabolic rate [65], whereas flapping forward flight costs about 5–6 times as much as gliding, or more.

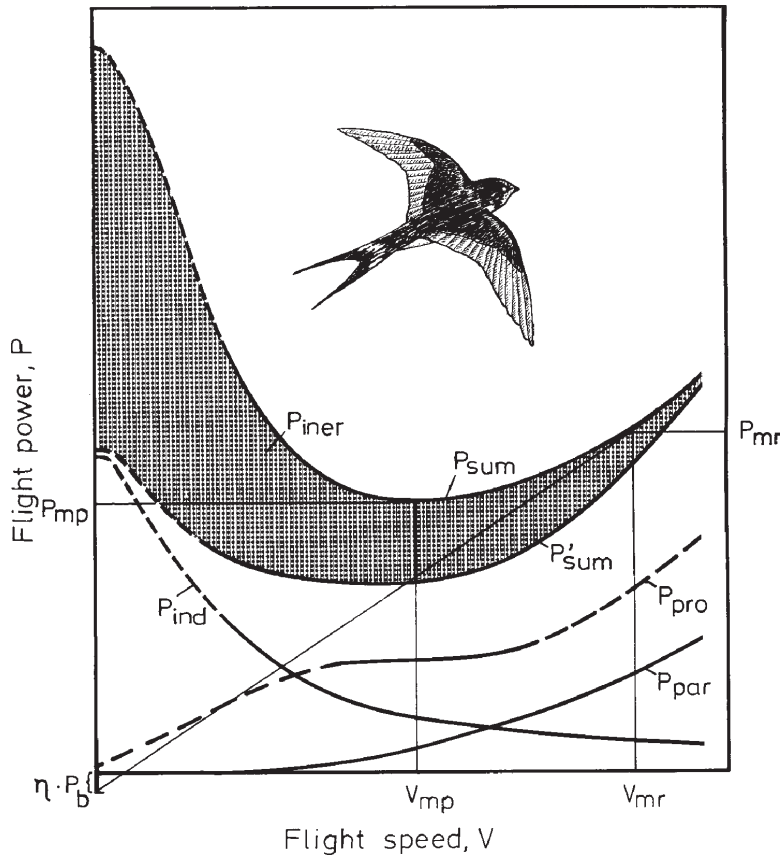

Figure 2: Mechanical power plotted against flight speed. P'_{sum} is the sum of the aerodynamic power components P_{ind} (induced power), P_{pro} (profile power) and P_{par} (parasite power). Adding the inertial power, P_{iner}, gives the total sum curve P_{sum}. The profile power is constant at medium speeds, according to Pennycuick's model [21], which is adopted here. P_{b} is the resting metabolic rate, P_{mp} is minimum power, P_{mr} is maximum range power, V_{mp} is minimum power speed, V_{mr} is maximum range speed and η is mechanical efficiency. From [6], courtesy of Blackwell Publishers.

The aerodynamics of gliding has been described by Pennycuick [21, 33] and Norberg [34, 66]. When gliding, the wings of animals leave behind a continuous vortex sheet that rolls up into a pair of wingtip vortices, as in fixed-wing airplanes. The lift force produced during steady gliding balances the animal's weight, but potential energy must be used to overcome the total drag. There is no thrust produced to balance these drag forces. Therefore, the gliding animal descends at an angle θ to the horizontal, determined by the resultant of lift and drag. This angle is established by the lift-to-drag ratio ($L/D = 1/\tan\theta$), called the *glide ratio* (Fig. 3). In steep glides, when $L/D < 1$, the animal is said to parachute. In a steady glide the lift and drag forces are

$$L = mg\cos\theta, \quad D = mg\sin\theta. \tag{16}$$

Gliding airplanes can reach a lift-to-drag ratio of 50:1, which means that the plane sinks 1 m for every horizontal transportation of 50 m. In birds the ratio ranges from 10:1 to 15:1 for birds

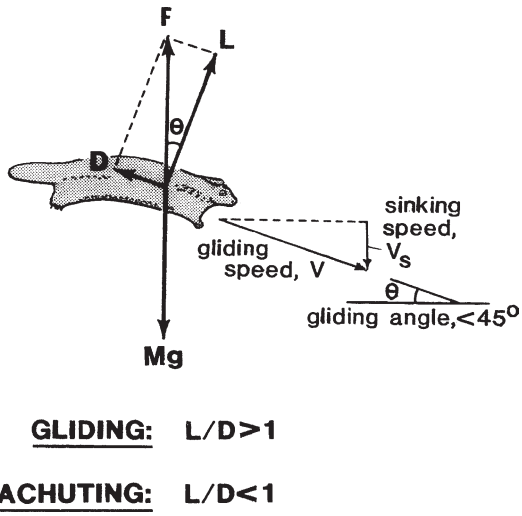

Figure 3: Forces acting on a gliding animal. When the gliding angle is larger than 45° the animal is said to parachute. Modified from [34].

of prey and vultures, and may reach 24:1 in albatrosses [67]. Gliding and parachuting also occur among fishes, frogs, reptiles, marsupials and squirrels, and have thus evolved independently in different animal classes. Some bats can glide but only for very short periods (but can use thermal or slope-soaring [68]). Experiments by Spedding [69] showed that the wake of a kestrel (*Falco tinnunculus*) in gliding flight consists of a *vortex sheet* shed from the trailing edge of the wings, which rolls up into a pair of trailing line vortices. The same vortex pattern occurs behind the wings of low-speed aircraft and can be described by lifting-line aerodynamic theory [70].

The graph of the sinking speed u_s plotted against gliding speed u_g (*glide polar*) summarizes the gliding performance (Fig. 4). The sinking speed in a glide is $u_s = u_g \sin\theta = Du_g/mg$. The minimum sinking speed depends on the relationship between wingspan and wing surface and on the polar curve for minimum drag. Inserting the equations for the various drag components, the sinking speed can be written as

$$u_s = 2kmg/\pi\rho b^2 u_g + 0.5\rho S u_g^3 (C_{Dpro} + C_{Dpar})/mg, \tag{17}$$

which describes a curve of the form

$$u_s = a_1/u_g + a_2 u_g^3. \tag{18}$$

The term a_1 is constant for a particular species and any air speed, whereas a_2 changes with air speed as C_{Dpro} varies with C_L (and thus speed). The gliding speed is obtained from eqns (4) and (8), which gives

$$u_g^2 = 2mg\cos\theta/\rho S C_L. \tag{19}$$

At small glide angles θ, $u_g \approx (2mg/\rho S C_L)^{1/2}$. To glide at the minimum gliding speed, the lift coefficient must be maximized. The speed for best glide, u_{bg}, when the animal is gliding with the minimum possible total drag, is the tangent to the curve described by eqn (17) (Fig. 4), and is

$$u_{bg} = (2mg/\rho S)^{1/2} [AR\varepsilon\pi(C_{Dpro} + C_{Dpar})]^{-1/4}. \tag{20}$$

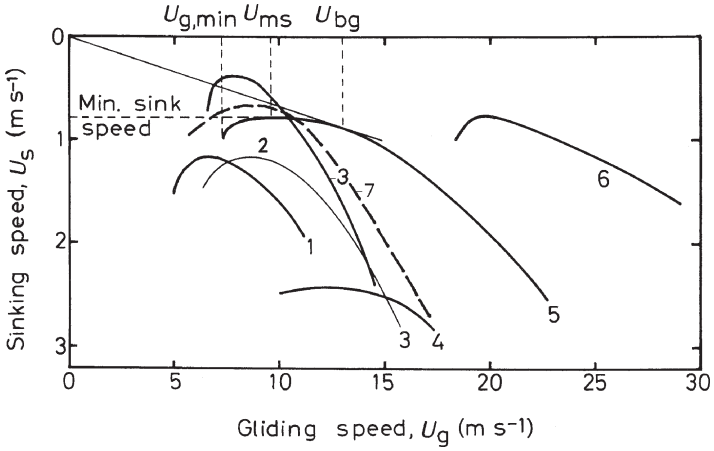

Figure 4: Glide polars displaying sinking speed versus gliding speed for some animals and for a motor glider: 1, dog-faced bat *Rousettus aegyptiacus*; 2, pterosaur *Pteranodon ingens*; 3, fulmar petrel *Fulmarius glacialis*; 4, pigeon *Columba palumbus*; 5, white-backed vulture *Gyps africanus*; 6, motor glider ASK-14; 7, Samoan flying fox *Pteropus samoensis* [34]. $u_{g,min}$ is minimum gliding speed, u_{ms} is minimum sink speed,u_{bg} is speed for best glide. Slightly modified from [34], courtesy of Springer-Verlag.

The term mg/S in eqns (18) and (19) is the *wing loading* and is of fundamental importance for flying animals and aircraft (see Section 7.2). Any characteristic speed will be proportional to the square root of the wing loading, so low gliding speeds are obtained with low wing loadings. The best glide speed, u_{bg}, increases with mg and decreases with wing area S and AR (and thus span b).

Soaring birds usually glide in vertical and horizontal air movements. Many large birds use soaring when searching for food, during migration and when commuting between roosting and foraging places. Some large bats (flying foxes) use soaring in slope lift and thermals [67].

Migrating birds often climb in thermals and then fly off to the next (Fig. 5). The bird must then fly in circles with low sinking speed. A narrow thermal can be used only if the bird can make tight turns without losing height faster than the air rises. Birds with low wing loadings can climb in weak and narrow thermals, because the radius r of a banked turn is directly proportional to the wing loading, $r \propto mg/S$ [71].

Albatrosses and petrels (family Procellariiformes, ranging in mass from 20 g to 9 kg) are the dominant flying birds of the open ocean in the southern hemisphere. They frequently use soaring, and classical theories of their 'dynamic' soaring include that gliding flight could be sustained by a gradient in the horizontal wind, increasing in strength with height [16, 72]. However, a simple calculation shows that a strong enough wind gradient can only be expected up to a height of about 3 m above the water surface, whereas albatrosses typically pull up to around 15 m [73]. The birds may instead extract pulses of energy from discontinuities in the wind flow ('gusts') due to flow separation over wave crests. Pennycuick [73] pointed out that the typical behaviour of albatrosses is to roll belly to wind to a very steep bank angle, as they pull up out of a separation bubble, when crossing a wave crest to windward. The ocean surface is covered with separation bubbles in winds of medium strength, which provide sources of kinetic energy for birds [74]. Pennycuick [73] further suggested that the forward-pointing nostrils of procellariforms serve as pitot tubes and that the large nasal sense organ can monitor dynamic pressure.

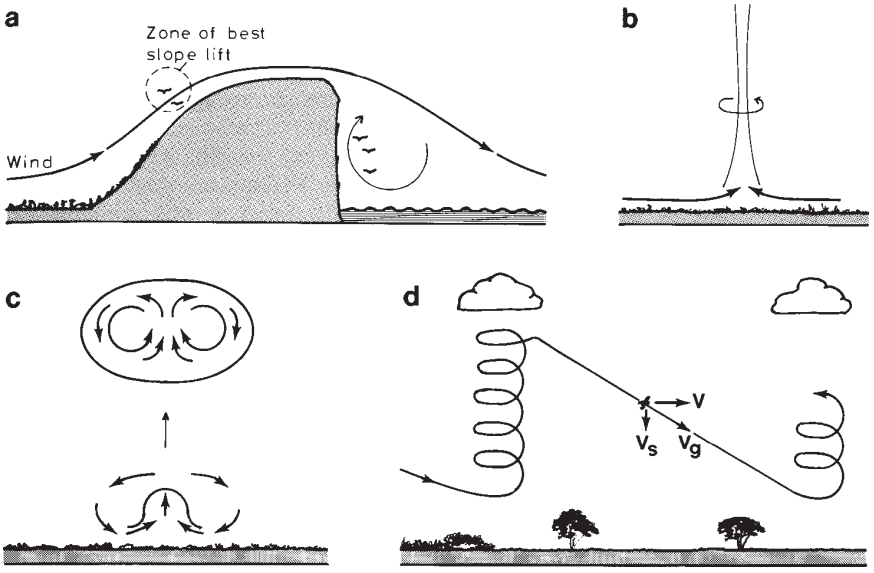

Figure 5: Different types of vertical air movements used by soaring birds. (a) Slope lift at smooth slopes or vertical cliffs. (b) Dust-devil, triggered from solar heating of the ground. (c) Vortex-ring, triggered from heated ground and rising as a distinct bubble. (d) Cross-country soaring by climbing in thermals and gliding in between them. V is the forward speed, V_g is the gliding speed and V_s is the sinking speed. From [34], courtesy of Springer-Verlag.

Pennycuick [49, 75] described two types of soaring wings, which allow exploitation in different situations (Fig. 6). The *long soaring wing* is found in birds that soar over the sea, such as gulls, albatrosses and frigate birds. The long pointed wing provides low induced drag and reduced profile drag, and the low wing loading permits the bird to exploit weak and narrow thermals. Birds that soar over land and take-off from the ground by flapping in the absence of wind have *short soaring wings*, i.e. short broad wings with slotted tips, such as storks, eagles, cranes, vultures and buzzards. They are also more manoeuvrable, since they can roll and yaw at higher angular velocities for a given speed [76]. Long wings reduce induced power and pointed wingtips reduce profile power.

5 Hovering

Hovering flight is performed by most insects and by many small birds and bats, although it is an expensive way of flying in the absence of a forward velocity component.

During hovering the body is usually tilted at a large angle to the horizontal, and as forward flight increases the body is held more horizontally. During the downstroke the wings are extended and swung downwards–forwards and the wingstroke angle usually depends on the flight speed. In the upstroke the wings are more or less flexed at the elbow and wrist to reduce drag, and in asymmetric hovering and slow flight the primaries usually separate to permit air to blow through [79]. In some birds and bats in very slow flight and take-offs there is a tip reversal ('flick phase') at the end of the upstroke [25, 80–83], which may produce a large thrust force, although this has not been confirmed by wake analysis [84].

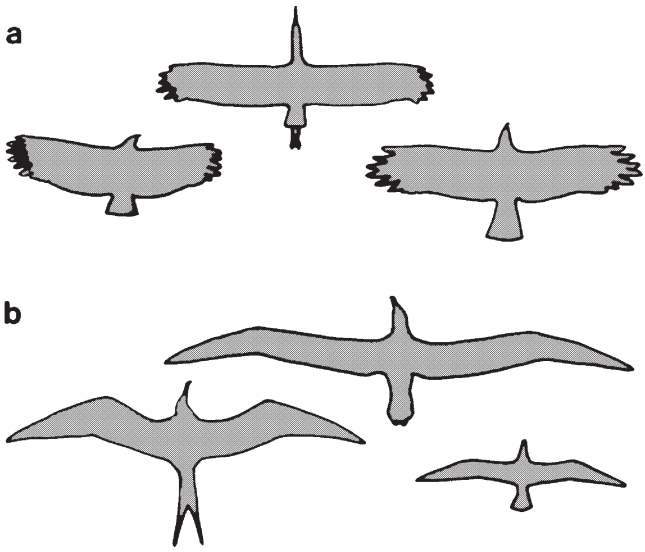

Figure 6: (a) Short soaring wings in (from left to right) a vulture, a stork and an eagle. (b) Long soaring wings in (from left to right) a frigate bird, an albatross and a gull. From [34], based on Pennycuick [77] and Herzog [78], courtesy of Springer-Verlag.

The wake in hovering animals depends on the effect of the up/backstroke. Birds that use *asymmetric hovering* (with flexed wings during the upstroke) may produce a stack of vortex rings, one for each single downstroke, while flying animals with *symmetric hovering* (hummingbirds and many insects) may generate two rings per wingbeat [28, 30, 85].

For birds using *symmetric* or *normal hovering*, when the wings are beating horizontally, the wings can be compared to the rotor blades of a helicopter. A simplification of a steady-state model is then the Rankine–Froude *momentum-jet theory* for an actuator disc. In this theory the wake is considered as a steady jet with a uniform axial velocity across any cross-sectional area and represents an ideal wake for a propeller with *minimum induced velocity*, w_i. The air reaches a final vertical velocity of $2w_i$ far below the animal (approximately one wingspan). The induced power required to generate an upward lift force equal to the weight is

$$P_{\text{ind,RF}} = mg\, w_i = (mg)^{3/2}/(2\rho S_d)^{1/2}, \tag{21}$$

where S_d is the disk area (the area of a circle with wingspan as diameters, $S_d = \pi b^2/4$). This gives a minimum value of the induced power. But, in animals the wake consists of periodic pulses and the actual induced power is then expressed as

$$P_{\text{ind}} = k\, mg\, w_i, \tag{22}$$

where the *induced factor* k is theoretically derived to be 1.1–1.2 for animal wings with horizontal stroke plane [31, 33] and about 1.4–1.6 for inclined stroke planes [29, 33]. Norberg *et al*. [86] measured the induced velocity in a nectar-feeding bat hovering with inclined stroke plane, and the obtained velocity corresponds to $k = 1.56$, which lies close to the theoretical values.

The forward flight velocity is zero in a hovering animal, but the flapping velocity is high. We therefore have a profile power component and the inertial power may be significant. The *profile*

power can be expressed as [23, 28, 29]

$$P_{\text{pro}} = 0.0166\,\mu\pi b^3 S C_{\text{Dpro}}\theta/\tau^2 T^3, \tag{23}$$

where μ is the muscle ratio, T is the wingstroke time and τ is the downstroke ratio (the time of downstroke divided by T). The muscle ratio is $(m_{\text{ms}} + m_{\text{mp}})/m_{\text{mp}}$, where m_{ms} is the mass of the muscles powering the upstroke and m_{mp} the mass of those powering the downstroke.

The significance of the *inertial power* has been intensively investigated by Weis-Fogh [23, 24]. One uncertainty is the extent to which inertial power is converted into useful aerodynamic power, which is not easily achieved in hovering and slow flight because of the low air velocity at the turning points of the wingstroke. The loss of inertial power would then be important unless kinetic energy can be removed and restored by some other means. The flexible wings of bats and the primary feathers of birds might increase the efficiency of transfer of the wing's kinetic energy to the air towards the end of the downstroke [34, 87]. At the end of the upstroke the downstroke muscles stretch and do negative work; this costs only about 20% of positive work and can be disregarded [23]. The inertial power is the total inertial work Q during one wingstroke times the wingstroke frequency,

$$P_{\text{iner}} = f\left[\int_{\gamma_{\min}}^{\gamma_{\max}} Q d\gamma + \int_{\gamma_{\max}}^{\gamma_{\min}} Q d\gamma\right], \tag{24}$$

where Q is the inertial bending moment, which equals the moment of inertia I times the angular acceleration of the wings, the fluid mass being excluded. Assuming that the wings oscillate in simple harmonic motion, the bending moment is [23, 24]

$$Q(t) = -2I\pi^2 f^2 \theta \sin(2\pi f t), \tag{25}$$

where t is the time. The moment of inertia depends on the distribution of the mass along the wing [34]. For small flying animals (insects), the viscous forces are large and the inertia of the wings will be increased by the mass of air attaching to them and accelerating with them (*wing virtual mass*), leading to an increase in wing mass [31, 88]. The possible effect for larger animals, such as birds and bats, is debated. The moment of inertia for one wing of birds and bats, with wing virtual mass excluded, has empirically been derived to be

$$I = 3.76 \times 10^{-3} m^{2.05} \quad \text{or} \quad I = 9.23 \times 10^{-3} b^{5.08} \tag{26}$$

for birds [89] and

$$I = 4.49 \times 10^{-3} m^{0.53} b^{2.15} S^{0.65} \tag{27}$$

for bats [76].

For a hovering 10.5-g bat, the total mechanical power was estimated to be 0.34 W, of which induced power made up ≈44%, profile power ≈1% and inertial power ≈55% (with zero elastic storage, [86]). With perfect elastic storage the inertial power would be zero. On including wing virtual mass the inertial power would increase by 50%. The mechanical power required to fly near minimum power speed for a 11.7-g bat was estimated to be only 0.14 W, of which induced, profile, parasite and inertial power made up about 28%, 39%, 4% and 29%, respectively.

During hovering, kestrels (*Falco tinnunclus*) perform rapid, rotational wing movements about the wing's long axis (along the span), and the wings are only slightly flexed during the upstroke. Lindhe Norberg [90] has suggested that this rotation may be a way to build up a vortex pattern during flight, increasing the mean lift coefficient.

6 Energy-saving flight

Except for using gliding and soaring there are several other ways of reducing power consumption during flight (see [34, 90] for reviews). Migrating birds use gliding, soaring and formation flight, and many other species use intermittent rest periods to keep muscle contraction dynamics close to optimum while obtaining a low mean power output. The different strategies are only briefly described here.

6.1 Intermittent flight

Intermittent flight includes *bounding flight* and *flap-gliding*. Finches, tits, wagtails and other smaller birds up to the size of the green woodpecker (*Picus viridis*, ≈0.1 kg) use bounding flight. It consists of flapping flight alternating with passive flight with folded wings, making the flying bird rise and fall in an almost ballistic path. During the passive phase the bird saves induced and profile drag, while during the flapping phase the wings must generate sufficient lift and thrust to sustain the bird through both phases.

Theoretically, *bounding* may reduce flight power at air velocities greater than about 1.1 times the maximum range speed, U_{mr}; a bird flying at 1.3–1.5 U_{mr} and with flapping time equal to bounding time would save about 17–35% of its energy expenditure [91–93]. But bounding has been observed at slower speeds than U_{mr} and even in hovering flight [26, 93, 94]. Bounding flight does not reduce the cost of transport below the minimum for steady flapping flight [93], so it cannot be explained solely as an adaptation to reduce power output, but instead to permit the flight muscles to work at maximum efficiency as much as possible. Birds should be able to increase their muscle efficiency by running the muscles near their maximum power output, which can only be done intermittently [33].

Larger birds (greater than about 0.1 kg) use *flap-gliding* (also called *undulating flight*; [92, 93]) to obtain intermittent rest periods. Their flight muscles can produce only little more power than what is needed for continuous flapping flight, which precludes them from using bounding flight. Flap-gliding is common in raptors, pelicans, ibises, shearwaters, albatrosses and many other medium-sized to large birds [33]. During the active phase the bird must exert more power than necessary to maintain its speed, so that it accelerates. It then stops flapping and glides on outstretched wings, still almost level but slowing down.

Rayner [93] calculated the power for a starling (*Sturnus vulgaris*) in flap-gliding. By flapping 25% of the time while climbing, and gliding downwards during the remaining 75%, theoretically, the power could be reduced by 14% at the minimum power speed and by 10% at the maximum range speed compared to steady flapping flight, and the minimum cost of transport could be reduced by about 11%. Rayner further suggested that birds with low wing loading and high aspect ratio, which require low flight cost, should be able to save still more by flap-gliding. This may explain why birds with low aspect ratios (passerines) or high wing loadings (ducks, auks) do not flap-glide [93].

Pennycuick [33] suggested that the main function of flap-gliding may not be an adaptation to reduce power output but to increase muscle efficiency. Flap-gliding birds must have slow muscle fibres for gliding flight, which requires isometric tension, in addition to the faster fibres for flapping flight. Both fibre types appear in large birds, whereas small birds have mainly fast fibres in their flight muscles [34].

Other intermittent strategies include the climbing–gliding behaviour of certain forest birds [95, 96], gliding reptiles and mammals, and probably of the ancient proto-fliers [97, 98].

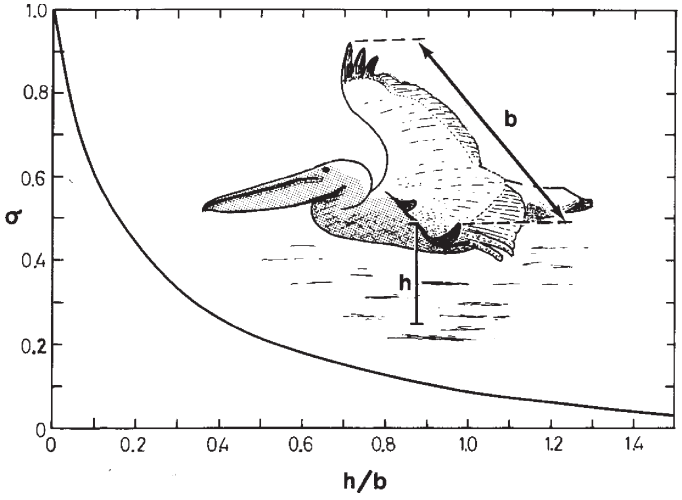

Figure 7: Reduction of induced drag (where $\sigma = 1$ means 100% reduction) against a non-dimensional index of the height above the surface (h/b, where h is height of wing plane above the surface and b is wingspan) From [34], courtesy of Springer-Verlag.

6.2 Ground effect

Birds flying close to the ground or water make use of the *ground effect*, known in aircraft theory to reduce the induced drag, which is high at slow flight speeds. The influence of a surface on birds flying close to it can be investigated by the method of images [99]. The image aerofoil will cause a reduction in the downwash angle and hence in the induced drag and power of the real aerofoil. There is a reduction of the flight speed also, resulting in a longer glide path.

The percentage reduction of induced drag and speed depends upon the ratio between the animal's height h above the surface and wingspan b, h/b, and is measured by an interference coefficient σ [100]. The induced power with ground effect is

$$P_{\text{ind,g}} = (1 - \sigma)P_{\text{ind}}, \tag{28}$$

and the corresponding minimum power and maximum range speeds are

$$U_{\text{mp/mr}} = (1 - \sigma)U_{\text{mp/mr}}. \tag{29}$$

When $h > b$ the value of σ is negligible, but σ exponentially approaches 1 (= 100% saving) as h approaches 0 (Fig. 7). Useful savings are made when $h < b/2$ [101]. By flying 7 cm above the water surface ($\sigma = 0.5$) and slightly faster than U_{mp}, the black skimmer (*Rynchops niger*) was estimated to reduce induced power by 50% and total mechanical power by 19% [102].

6.3 Formation flight

Some migrating birds, such as geese, swans and cranes, fly in *formation flight*, which theoretically reduces the induced power (Fig. 8a and b). The theory for formation flight has been described by Lissaman and Shollenberger [103] and Higdon and Corrsin [104], and summarized by Norberg [34]. A flying bird in a flock is thought to exploit the upwash created by the wingtip of the adjacent

bird diagonally in front of it and the same effect as flying in an upcurrent is obtained (Fig. 8d). This decreases the required strength of the self-induced downwash and the net induced drag of each wing. The induced power depends critically on downwash distribution and thus on spanwise loading. Heppner [105] distinguished between two-dimensional *line formation* (Fig. 8a) and three-dimensional *cluster formation* (Fig. 8b), and found that the energy saved by each individual will depend on the geometry of the formation and on the relative positioning of the wingtips (Fig. 8c).

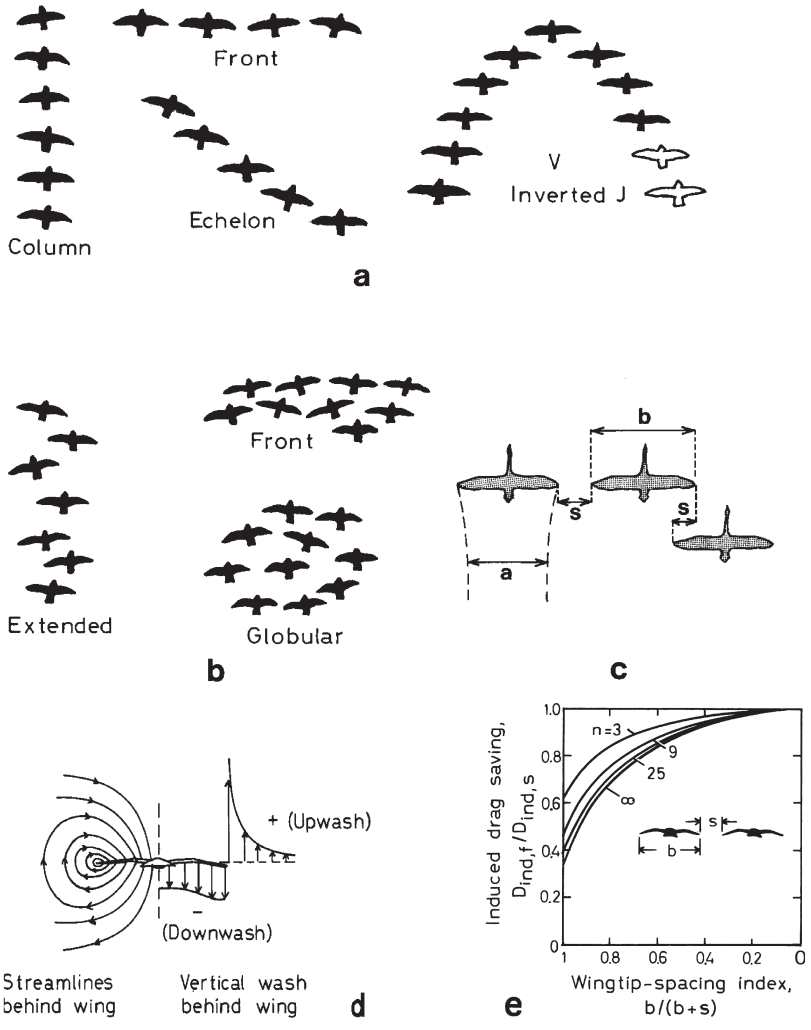

Figure 8: (a) Line formations and (b) cluster formations [105]. (c) Wingtip spacing s and effective wingspan a (the distance between the two wingtip vortices at some distance behind the bird) of birds flying in flock formation. (d) Flow streamlines (left) and vertical velocity vectors of the induced flow (right). (e) Induced drag saving as a function of wingtip spacing s. $D_{\text{ind,f}}$ is the induced drag of a bird in formation flight and $D_{\text{ind,s}}$ is that in solo flight (data from [103]). From [34], courtesy of Springer-Verlag.

Lissaman and Shollenberger [103] estimated up to 71% savings of the induced power for a bird in formation flight. Figure 8e shows the induced drag saving as function of wingtip spacing s in formations with 3, 9, 25 and an infinite number of birds. Large savings would occur only when the spacing is small and when there are many birds. At the speeds used during migration (theoretically U_{mr}; [21]), the induced power is only a small part of the total power, so the maximal saving would become about 14% of the total power [34].

7 Scaling of flight parameters

Using scaling it is possible to predict how a length, an area or a volume (such as a mass) varies with some other parameter for flying animals. Empirical allometric relationships allow exploration of how different mechanical, physiological and ecological constraints change in importance with body size and wing or tail form. Regression lines based on morphological or physiological variables can provide general norms for animal groups and allow identification of deviations from the norm that may indicate adaptations to different biological niches and/or habitats [34, 35, 41, 106, 107–109]. With dimensional analysis one can thus compare and correlate relations between species with pronounced size differences. Allometric scaling is also widely used for estimation of body masses of extinct animals from skeleton data compared with sizes of extant animals.

Geometric similarity (isometry, where any area $\propto$ any length squared and any mass $\propto$ any length cubed) is often assumed in theoretical models to calculate how speed, power and cost of transport scale with body mass of flying animals [18, 21, 34, 35, 108–110], although we know that all birds are not geometrically similar. But deviations from isometry are small for most single bird groups; therefore, relationships of speed, power and cost of transport to body mass based on geometric similarity can be regarded as good approximations. The various equations give us an understanding of how changes in flight morphology and behaviour affect flight performance, although we do not get exact estimates.

7.1 Wingspan and wing area

Greenwalt [106] showed that wingspan and wing area in birds increase faster with increasing body mass than predicted by geometric similarity. In all birds, except hummingbirds, the wingspan increases as $b \propto m^{0.39}$ and the wing area as $S \propto m^{0.72}$; but in hummingbirds wingspan and wing area scale as $b \propto m^{0.53}$ and $S \propto m^{1.04}$. For isometry these exponents would be 0.33 and 0.67, respectively. Large flying animals thus have proportionately longer wings of larger areas than small ones. In bats, these parameters scale as $b \propto m^{0.32}$ and $S \propto m^{0.64}$ [3], in ancient bats as $b \propto m^{0.28}$ and $S \propto m^{0.48}$ [111], and in pterosaurs as $b \propto m^{0.40}$ and $S \propto m^{0.79}$ [34, 112]. There is, however, a large variation among different groups of both birds and bats (Fig. 9).

7.2 Wing loading and aspect ratio

Wing loading gives an indication of the wing size and is a ratio of a force (weight) to an area, and is thus equivalent to a pressure. It is related to the mean pressure force over the wings and therefore $mg/S \propto U^{1/2}$. For geometrically similar animals, wing loading should scale with body mass as $mg/S \propto m^{0.33}$, which is also found in megachiropteran bats (flying foxes). The wing loading thus increases with the size of the animal, which has an influence on flight performance.

Because wingspan and wing area increase more with increasing body mass in birds (with hummingbirds excluded) than would be expected for isometry, their wing loadings actually increase

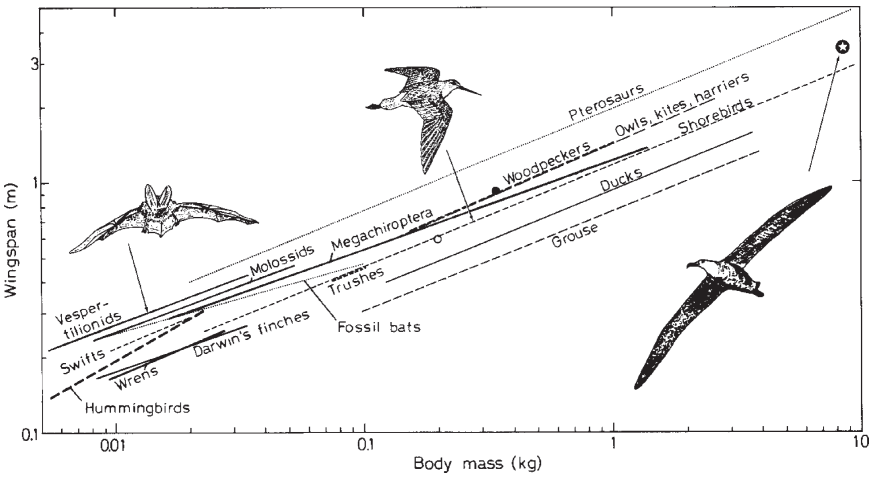

Figure 9: Wingspan versus body mass for some animal groups. Filled circle shows the span for a fossil bat (*Archaeopterus*), open circle that of *Archaeopteryx* and the star that of the wandering albatross (*Diomedea exulans*). From [34], courtesy of Springer-Verlag.

less with body mass ($mg/S \propto m^{0.28}$). This was also the case for pterosaurs ($mg/S \propto m^{0.22}$). Surprisingly, there is no change with body mass in hummingbirds ($mg/S \propto m^{-0.04}$), and nearly so in gliding vertebrates (Fig. 10). Manoeuvrability depends on wing loading, because it depends on the minimum radius of turn r which is directly proportional to the wing loading [71]. Wing loading in extant (modern) birds ranges from about 17 N/m^2 in small hummingbirds (2.3 g) to 230 N/m^2 in the Whooper Swan (10 kg).

The non-dimensional *aspect ratio* reflects the shape of the wings and is interpreted as a measure of the aerodynamic efficiency. A high aspect ratio wing has a low induced drag and is therefore advantageous for gliding and slow flapping flight, and the lift-to-drag ratio (= glide ratio) increases with increasing aspect ratio [35, 111]. Furthermore, the agility and manoeuvrability improves with smaller aspect ratio.

Aspect ratio should be constant in geometrically similar animals of different sizes, since $\mathrm{AR} = b^2/S \propto l^2/l^2 = l^0$. Hummingbirds have aspect ratios almost independent of size, whereas for other bird groups the ratio increases slightly with size, the exponent varying between 0.05 for smaller birds and 0.1 for larger birds [107]. In microchiropteran bats the exponent is 0.11, while in the megachiropteran bats it is 0.21. In pterosaurs the exponent has been estimated to be 0.10 [35, 112]. Figure 11 shows the aspect ratio plotted against body mass for various flying animals. In modern birds the aspect ratio ranges from 4 in some galliforms and tinamous to 18 (or higher) in albatrosses.

7.3 Flight speed and power

Larger birds have to produce more power from each gram of muscle than do smaller ones, and they are obliged to fly faster because of their higher wing loadings [21]. Assuming geometric similarity and that the lift coefficient is constant, any characteristic flight speed should vary with the square root of the wing loading, $U \propto (mg/S)^{1/2} \propto m^{1/6=0.17} \propto l^{1/2}$. Thus, if a bird is geometrically similar to another bird but has x times the wingspan, then it should fly $x^{1/2}$ times as fast.

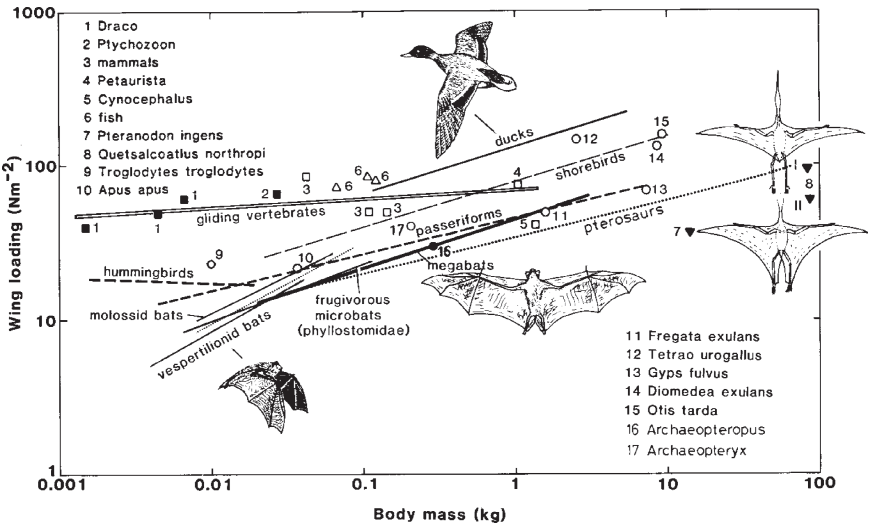

Figure 10: Wing loading versus body mass for some gliding and flying animals. From [34], with data from animals numbered 1–6 from Rayner [113], courtesy of Springer-Verlag.

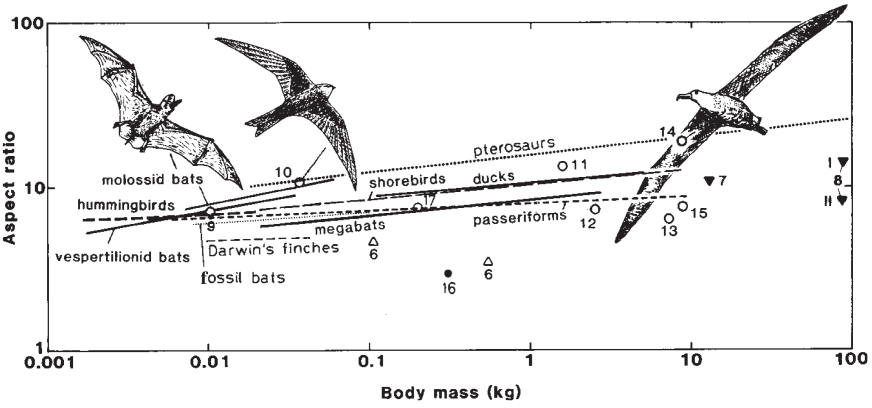

Figure 11: Aspect ratio versus body mass for some groups of animals. The numbers refer to the animals as identified in Fig. 10. From Norberg [34], courtesy of Springer-Verlag.

In steady horizontal flight the muscle power required to fly [eqn (11)] is $P_{\text{mech}} = DU = mgU(D'/L') \propto m^{7/6=1.17} \propto l^{7/2}$ [21]. If a bird weighs twice as much as another geometrically similar bird but has x times the wingspan, then it should require $2^{7/6} = 2.24$ times as much power to fly at any characteristic speed under similar conditions.

Based on Rayner's [108] theoretical models, and empirical data for bats from Norberg and Rayner [3] (see also [114]), the following expressions for the minimum power (P_{mp}) and the maximum range power (P_{mr}), the related speeds (U_{mp} and U_{mr}), and the dimensionless cost of transport (C_{mr}) were derived:

$$P_{\text{mp}} = 10.9m^{1.19} = 24.0m^{1.56}b^{-1.79}S^{0.31}, \tag{30}$$

$$P_{\text{mr}} = 15.0m^{1.16} = 27.2m^{1.59}b^{-1.82}S^{0.28}, \tag{31}$$

$$U_{\mathrm{mp}} = 8.96m^{0.21} = 6.58m^{0.42}b^{-0.48}S^{-0.15}, \tag{32}$$

$$U_{\mathrm{mr}} = 11.8m^{0.21} = 8.71m^{0.42}b^{-0.50}S^{-0.14}, \tag{33}$$

$$C_{\mathrm{mr}} = 0.105m^{-0.036} = 0.319m^{0.11}b^{-1.26}S^{0.47}. \tag{34}$$

The inertial power is not included in the model giving these expressions. The small discrepancies from expected coefficients depend on the wingspan and the wing area and are not geometrically similar in birds of different sizes.

7.4 Wingbeat frequency

In geometrically similar animals the maximum frequency should vary with the negative one-third power of the body mass, $f_{\max} \propto m^{-1/3=-0.33}$ [115]. The minimum wingbeat frequency depends on the wing loading and is associated with the need to provide sufficient lift and thrust during hovering and slow flight, $f_{\min} \propto m^{-1/6=-0.17}$ with isometry [18, 21]. Estimation of the flapping frequency in birds, in general, shows that it varies with body mass according to $f = 3.87m^{-0.33}$ and according to $f = 3.98m^{-0.27}$ when hummingbirds are excluded [108].

Pennycuick [116] used multiple regression and dimensional analysis on empirical data for 47 bird species with diverse mass and wing forms and showed that the *natural* wingbeat frequency may be estimated by

$$f = (mg)^{1/2}b^{-17/24}S^{-1/3}I^{-1/8}\rho^{-3/8}. \tag{35}$$

This equation predicts that if, for example, the body mass were to change in the course of a flight in one individual (at the same air density), it should cause the wingbeat frequency to change in proportion to the square root of the mass, which was also found in experiments conducted on two bird species flying in wind tunnel [59].

Nudds *et al*. [46] used the Strouhal number, $\mathrm{St} = fa/U$, to derive a reliable prediction of variables and test their results with Pennycuick's equation, using data from Taylor *et al*. [117]. In birds of various sizes and morphology the wingstroke angle θ scales with wingspan as [118]

$$\theta = 67b^{-0.24}. \tag{36}$$

This equation was used to predict θ for 60 new species, for which they could find measurements of f and U in cruising flight. The following relationship was then obtained,

$$f \approx \mathrm{St}\ U/b \sin(33.5b^{-0.24}), \tag{37}$$

where St is shown to fall in the range $0.2 < \mathrm{St} < 0.4$. This equation thus requires knowledge of only cruising speed and wingspan, but they must covary. The authors noted that the coincidal scaling of stroke angle with span is peculiar to birds. Within a narrow range of St the product of frequency and amplitude should scale as $fa \propto m^{1/6=0.17}$ [46].

The predicted wingbeat frequency can also be used to estimate the mechanical power required to fly, for the mechanical power produced by a particular flight muscle is directly proportional to the contraction frequency [115]. With isometry, the maximum power available to fly should be proportional to $m^{2/3=0.67}$ and the minimum power required to $m^{7/6=1.16}$ [21]. Muscle strain ε (change in muscle length relative to estimated length) and stress σ (force per unit cross-sectional area) are then assumed to be independent of body mass, and so is the mass-specific work $\varepsilon\sigma/\rho_{\mathrm{m}}$, where ρ_{m} is the muscle density. The mass-specific power required to fly, P^*_{m}, at comparable velocities in geometrically similar birds should thus scale in proportion to $P^*_{\mathrm{m}} \propto m^{0.16}$ [21].

However, changes in drag with changing Reynolds number could result in P_m^* scaling between m^0 and $m^{0.16}$ [118].

This has been tested in studies of take-off power estimates in insects and birds. For geometrically similar animals Marden [119] showed, with a multivariate regression, that lift per unit muscle power in insects and vertebrates taken together would scale with body mass as $m^{-0.16}$, which means a decline in flight ability with increasing body mass. Tobalske and Dial [120] used whole-body kinematics for four birds in the grouse family Phasianidae and estimated that pectoralis mass-specific take-off power decreased in proportion to $m^{-0.26}$ (independent contrast) or $m^{-0.33}$ (species data) and that it was directly proportional to wingbeat frequency. They found that muscle strain ε increased with body mass as $m^{0.23}$, which may be due to increase in both fractional lengthening and fractional shortening in the pectoralis muscle, but there were no significant correlation between stress σ and body mass. Askew *et al.* [121] estimated the mechanical power output of five species among Phasianidae and found no significant scaling of mass-specific power output with body mass, but there was a tendency for power to decrease in the largest species (in proportion to $m^{-0.14}$).

7.5 Upper and lower size limits

For geometrically similar animals, the power available for flight depends upon the flapping frequency, which determines the upper and lower size of flying vertebrates. Pennycuick [18, 21, 110] presented models for how big a bird can fly and what restricts or permits a flying animal to use a certain flight mode. Minimum and maximum wingbeat frequency lines converge as body mass increases. The lines meet at a maximum body size (12–15 kg in birds and about 1.5 kg in bats), above which the animals cannot beat their wings fast enough to achieve the lift needed for aerobic horizontal flight (Fig. 12). The power available from the flight muscles cannot produce the power required to fly at the minimum power speed. But the world's largest known flying bird, *Argentavis magnificens*, and the largest found pterosaur, *Quetzalcoatlus northropii*, may have weighed more than 75 kg (see Section 1). On the other extreme, very small birds and bats (< 1.5 g) cannot develop the power required to fly, because vertebrate muscles cannot contract at the high rate needed. Insects do not have this limit as their fibrillar muscle can operate at much higher frequencies [21]. The smallest bird, the hummingbird, weighs about 1.5 g and the smallest bat about 1.9 g.

For geometrically similar animals, the power required for flight should scale as $P_r = P_{mech} \propto m^{7/6}$ [eqn (11)] and the power available from the flight muscles as $P_a = m_m Q_m^* f_{max} \propto m \times m^0 \times m^{-1/3} \propto m^{2/3}$ [21], and these power lines converge and meet at the maximum body size. The ratio of the power available from the flight muscles to the power required to fly at the minimum power speed is called the *power margin* [21]. Small birds and bats have a large power margin and can use a range of flight modes, whereas very large flying animals are limited to fly horizontally and to use soaring and gliding flight as much as possible, and they usually have to take-off by jumping from a height, or by skittering on water surfaces at take-off runs. Hovering and manoeuvring are thus restricted to smaller animals.

8 Wing and tail design

Birds and bats show a wide range of adaptations to flight. The various flight modes are associated with different wing designs. Wing loading and aspect ratio, quantifying the size and shape of the wings, are widely used both in aircraft engineering and in studies of animal flight [3, 108]. The tails of birds are also important because they vary as much as their wings, or even more [63].

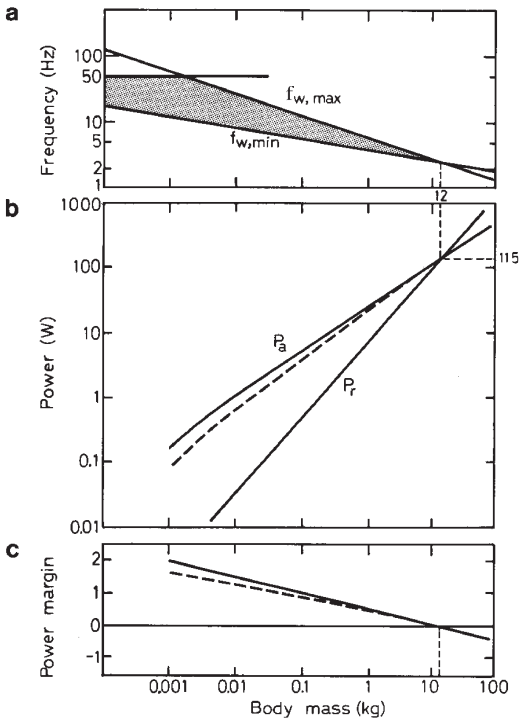

Figure 12: (a) Maximum and minimum wingbeat frequencies, $f_{w,max}$ and $f_{w,min}$, converge as mass increases. The stippled area is available to vertebrate fliers. The horizontal line is approximate and reflects the minimum time taken to reset the muscle after contraction. (b) Power required to fly, P_r, at minimum power speed and the power available, P_a, from aerobic (continuous line) and anaerobic (broken line) flight muscles. (c) Power margin for vertebrate fliers. From [34], modified from [110], courtesy of Springer-Verlag.

The tail is important in maintaining stability over a range of flight speeds and in generating lift to help with turning and slow flight, although it also reduces a bird's overall lift-to-drag ratio.

But bird morphology does not always follow biomechanical laws. Display features in birds, such as a long tail, most often mean increased costs for flight. Selection pressures for various demands are often conflicting, necessitating compromise adaptations [34]. The relationships between foraging strategy, flight performance and wing shape in birds have been discussed in several papers [6, 21, 33, 70, 108, 122–126].

8.1 Wing design

Aerodynamic performance can be improved by making the wings longer and thinner. The aspect ratio is around 20 in high-performance gliders whereas aeroplanes used in aerobatics have short broad wings for high manoeuvrability. But very long wings are more vulnerable to breakage, are impractical in cluttered environments and limit take-offs from the ground.

Certain combinations of wing loading and aspect ratio permit a flying animal to adopt particular flight modes and foraging strategies [127]. Figure 13 shows plots of aspect ratio versus a mass-compensated measure of wing loading ('relative wing loading', RWL = $m^{2/3}/S$ [128])

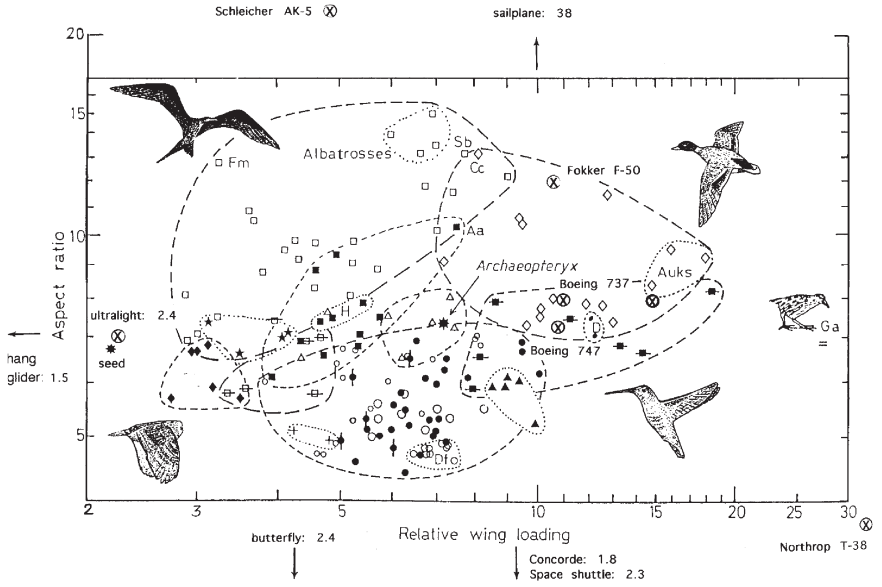

Figure 13: Aspect ratio (AR $= b^2/S$) versus relative wing loading (RWL $= m^{2/3}/S$) in various fliers. Open squares: various seabirds and raptors—*Diomedea, Milvus, Circus, Pandion, Larus, Sterna, Pelecanus, Fregata* (Fm = *Fregata magnificens*); filled squares: swifts (Aa = *Apus apus*), hirundines, falcons (*Falco, Accipiter*); filled squares with line: hummingbirds; open squares with line: vultures, *Buteo*, eagles; stars: cranes, storks, herons; plus sign: flycatchers; open rhombuses: loons, mergansers, geese, swans, ducks, auks; filled rhombuses: owls, many raptors; open circles: smaller passerines; filled circles with line: treecreepers, nuthatches, woodpeckers; filled circles: warblers, wrens, *Parus*; open triangles: waders; filled triangles: galliforms (Ga = *Gallirallus australis*); Dfo, Darwin's finches. From [128], courtesy of Wiley-Liss, Inc.

for modern birds, *Archaeopteryx*, some aircraft, a hang-glider, a sailplane, a butterfly and a seed. Aircraft are, of course, not limited by power requirements in the same way as animals, and are allowed to have values outside those for animals that have to beat their wings to produce thrust. But they are marked for comparison. It is then more appropriate to compare gliding vehicles with gliding and soaring animals. Jumbo jets have aspect ratios around 7 and Concorde as low as 1.8.

Low total flight power is obtained with a high aspect ratio, particularly in combination with a low wing loading since this permits slow flight with ensuing low wing profile and parasite powers. A high RWL means that the flyer has to fly fast for its size to obtain the necessary lift and its manoeuvrability is low [34, 90, 128].

Species with long, high-aspect ratio wings have low or average wing loadings, and their flight is slow and inexpensive. These birds (many seabirds, the swifts and swallows) normally use continuous foraging and cruising flights in open spaces. High performance sailplanes, such as Schleicher AK-5, are found in the upper left part of the diagram but with higher aspect ratio than for albatrosses. Wingtip shape varies among species and affects the flight mode. For a given span a rounded wing produces an elliptic transverse lift distribution, which yields a minimum induced drag plus a constant C_L along the wingspan. The tapered aft-swept tips in swifts can extract more

energy from the vortical wake and produce less drag for given lift than a lifting surface with an elliptic bound-circulation distribution which occurs in more rounded wings [129].

Species with high RWL and short wings but still of high aspect ratios are adapted to fast and rather expensive flight. Commuting and migrating species are found among these, such as loons, mergansers, geese, swans and ducks. Most of these species have to skitter on the water before taking-off. Auks have lower aspect ratios and still more costly flight. Birds with higher wing loadings have lost their ability to fly, such as the penguins, ostriches, the emu and the Australian rail.

Birds with low aspect ratio and low RWL include owls, broad-winged raptors, cranes, storks and herons. These birds have broad slotted wingtips which act to delay stall, reduce induced drag via prevention of too large wingtip vortices and increase lift [130–135]. Low wing loadings permit slow and manoeuvrable flight and aid in decreasing the flight costs. Ultralights and maple seeds come closest to owls among birds, but have even lower RWLs.

Species with average RWL ($=5-8$) and low aspect ratio include many small passerine birds. They have fairly expensive flight and are usually perchers and spend much of their foraging time walking, climbing, clinging and hanging.

There are not many flying species with a high RWL combined with a low aspect ratio, because this requires very high energy costs for flight. Gallinaceous birds belong to this category, and the largest of these spend a lot of time on ground.

The wing dimension of *Archaeopteryx* was about the same as for pigeons, starlings, thrushes and many waders, with a RWL about average for modern birds and its aspect ratio slightly higher than average.

8.2 Tail form

The tails of birds can take intricate costly shapes in sexually dimorphic species [136], but in most birds they have an aerodynamic function. A tail reduces a bird's overall lift-to-drag ratio, but it is important in maintaining stability over a range of flight speeds [34, 63, 133, 137, 138] and in generating lift to help with turning and slow flight [137, 138]. Open-country birds selected for high lift-to-drag ratio have relatively short tails, whereas birds that need high manoeuvrability in order to feed aerially or avoid collisions in cluttered environments have longer tails [139].

Most birds have a tail where the outer feathers are longer than the inner ones, and when spread the tail will acquire a shape that is similar to a delta wing. Thomas [63] applied slender lifting-surface theory on a bird's tail, which has been used to model delta-winged aircraft, such as the Concorde. According to this theory the flow over the tail is three dimensional with transverse flow moving around the leading edges from below to the dorsal surface. The lift generated by the tail is proportional to the square of the tail's continuous span but unaffected by its shape. Only the part of the tail in front of the point of the maximum width of the spread tail is aerodynamically functional. Any area behind this point will cause drag due to friction. Therefore, any tail with highly elongated inner feathers (evolved as sexual ornaments) are highly drag producing [6], whereas the elongated outer tail streamers in the barn swallow (*Hirundo rustica*) produce lift and increase manoeuvrability during flight [138]. However, Evans *et al*. [140] tested the delta-wing theory on barn swallows flying in a wind tunnel and showed that the predictions are not quantitatively well supported. The authors suggested that a modified version of the delta-wing theory or a new theory is needed to adequately explain the way in which morphology varies during flight.

The trailing edge of a bat's wing membrane is continuous with that of the tail membrane, so the total flight silhouette becomes almost triangular. During flapping, the legs move downwards and upwards with the wings, which is most pronounced in slow flight [25, 34, 80]. Thus, the tail

membrane is more active during flapping flight, and may produce more lift per unit area than the bird tail.

8.3 How changes of shape and mass affect the power curve

The wingspan, wing area, tail spread and tail angle of attack can change substantially during a wingbeat and with flight speed, and the geometry of the lifting surfaces adopted during manoeuvres or accelerating flight can differ substantially from that in steady flight. The bird tail can reduce the power required for flight at low speeds, and reducing the wingspan can reduce the power required for high speed flight [137, 141–143].

Norberg [6] showed how a long tail and changes in body mass in birds theoretically would change the power curve. A long soft tail, like the one in the long-tailed widowbird (*Euplectes progne*), would increase parasite power extensively as compared with a similar-sized bird with a 'normal' tail. Minimum power (P_{mp}) and maximum range power (P_{mr}) are higher, and the corresponding speeds (U_{mp} and U_{mr}) are lower in the long-tailed bird than in the short-tailed bird. Long-tailed birds should thus fly slower than the short-tailed birds to save energy.

An increase in weight causes an increase of the wing loading, which in turn requires higher flight speed for the production of enough lift in slow flight. For a 10-g bat or bird a 25% increase in body mass would increase P_{mr} and P_{mp} by 25–30% and U_{mr} and U_{mp} by 5–10%. A 50% increase in body mass, which is not unusual before migration in birds, would increase P_{mr} and P_{mp} by 45–50% and U_{mr} and U_{mp} by 20–25% [6].

A bat or bird carrying prey in the beak/mouth or claws should use about the same speed to minimize flight costs as when flying without prey. An increase of the induced power alone would increase total power and optimal speeds, whereas an increase of parasite power alone would increase total power but decrease the optimal speeds [6]. Total power would increase but the opposing tendencies regarding the speeds may instead cause the optimal speeds to remain about the same.

8.4 Some lift-enhancing characteristics

Flapping flight always includes phases with unsteady flow, which can take the form of intense local vortices shed from the wing's leading edge or the wingtips, or vortices trapped on or close to the wings [144, 145]. A main problem for flying animals and aircraft therefore is to obtain enough lift in slow flight. This is important during take-off and landing and for many birds and bats that take prey in the air and/or fly among vegetation.

One way to increase lift is to increase *camber* (anteroposterior curvature) or the angle of incidence of the wings (at the expense of higher drag). A problem is when the air becomes turbulent over the wing, which can cause a sudden fall of the lift and increase of the drag. But there are several ways to reduce turbulence and thereby delay stall, in aircraft as well as in flying animals. Such high-lift devices include the use of *flaps* and/or *leading-edge slats* to increase the maximum lift coefficient above that for the reference aerofoil itself. Various flap concepts have been described by Kuethe [146] and reviewed by Lindhe Norberg [128], and so they are not discussed further here.

Cone [15, 16] suggested that the bent wingtip feathers in birds may act as *endplates*, which inhibit airflow around the wingtip and reduce the effect of the shed vortices. Such endplates can be seen in small motor planes (Fig. 14) as well as in larger aircraft.

In owls the leading edge feather has barb hooks, forming a fringe along the front of the anterior vane [42]. In some range of angles of incidence the air flowing through the teeth of the comb

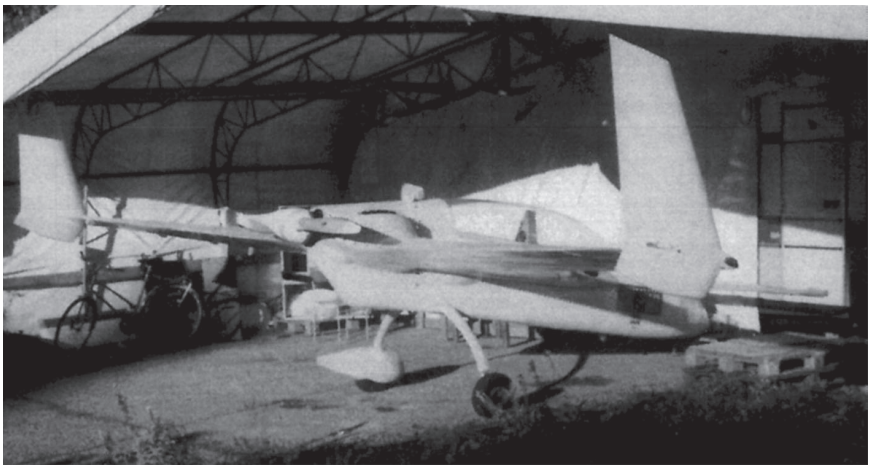

Figure 14: A small aeroplane with large endplates at the wingtips. Photo: U.M. Lindhe Norberg.

becomes turbulent, thus acting as *turbulence generators* of the boundary layer. By making the boundary layer turbulent the flow can remain attached to the surface at higher angles of attack than with a non-turbulent boundary layer, and hence a larger lift coefficient can be attained [42, 147]. This arrangement also suppresses the boundary layer noise and makes the flight silent which is important to night hunters for their acoustic localization of and approaching a prey. Hairs and projecting skeleton parts in the bat wing near the leading edge may also act as turbulators of the boundary layer [49, 148]. Dragonfly wings have pleats and hairs and saw teeth along the leading edge and spades for the same reason [42].

9 Conclusions

Flying animals have, over millions of years, evolved sophisticated morphological and physiological adaptations to life in air, and we are often surprised at how various characteristics can be so ingenious. Darwinism has taught us that evolution through natural selection favours those individuals that are the most adapted to their environment. Birds, like bats, are adapted to different flight behaviour, which means that there is a large variation in wing form and structure. Because there often are conflicting selection pressures for high flight performance, the optimal morphology can be difficult to interpret. But by combining looks and behaviour in a flying animal with physical laws we can grasp the evolution and adaptation of a particular characteristic.

During the last few decades the science of engineering has provided considerable insight into biological adaptations. We often find that structures in nature and in engineering follow the same mechanical laws to create, for example, strength, stability and high performance. But studies on structures, forms, organs and processes in nature have also helped the engineer to find solutions to various problems, such as in the design of micro air vehicles [128].

The flapping wings and moveable tail in birds and bats make their flight more complicated than for aeroplanes with fixed wings, but increase their ability to make manoeuvres and to change wing form to meet different flight conditions.

Predictions of flight behaviour and performance can be made from dimensional analysis. Regressions of wing morphology and aerodynamic characteristics make it possible to compare

animals of different sizes with each other and to understand how different constraints change in importance with size and wing form.

References

[1] Schmidt-Nielsen, K., *Scaling: Why is Animal Size so Important?* University Press: Cambridge, 1972.

[2] Vizcaino, S.F. & Farina, R.A., On the flight capabilities and distribution of the giant Miocene bird *Argentavis magnificens* (Teratornithidae). *Lethaia*, **32**, pp. 271–278, 1999.

[3] Norberg, U.M. & Rayner, J.M.V., Ecological morphology and flight in bats (Mammalia; Chiroptera): wing adaptations, flight performance, foraging strategy and echolocation. *Philosophical Transactions of the Royal Society London B*, **316**, pp. 335–427, 1987.

[4] Rayner, J.M.V., Bounding and undulating flight in birds. *Journal of Theoretical Biology*, **117**, pp. 47–77, 1985.

[5] Evans, M.R. & Thomas, A., The aerodynamic and mechanical effects of elongated tails in the scarlet-tufted malachite sunbird: measuring the cost of a handicap. *Animal Behavior*, **43**, pp. 337–347, 1992.

[6] Norberg, U.M., How a long tail and changes in mass and wing-shape affect the cost for flight in animals. *Functional Ecology*, **9**, pp. 48–54, 1995.

[7] Prandtl, L. & Tietjens, O.G., *Fundamentals of Hydro- and Aerodynamics*, Un. Engin. Trust., 1934, Reissued by Dover: New York, 1957.

[8] Tikkanravov, M.K., Polet ptits i mashiny s mashuschimi kryl'yami [The flight of birds and machines with flapping wings]. *ONTI*, 1937.

[9] Golubev, V.V., Mekhanizm obrazovaniya tyagi mashushchevo kryla [The mechanism of thrust formation in a flapping wing]. *Trudy nauchn. konferentsii, VVIA*, 1944.

[10] Golubev, V.V., Tyaga maschuschchevo kryla [The thrust of a flapping wing]. *Izvest. Akad. nauk*, **5**, *OTN*, 1945.

[11] Brown, R.H.J., The flight of birds. The flapping cycle of the pigeon. *Journal of Experimental Biology*, **25**, pp. 322–333, 1948.

[12] Brown, R.H.J., The flight of birds. II. Wing function in relation to flight speed. *Journal of Experimental Biology*, **30**, pp. 90–103, 1953.

[13] Gladkov, N.A., *Biologichyeskaya osnovyi polyeta ptits* [*Biological Principles of Bird Flight*], Nauka: Moscow, 1949.

[14] Vinogradov, I.N., *The Aerodynamics of Soaring Bird Flight*, Royal Aircraft Establ.: Farnborough, 1960.

[15] Cone, C.D., Thermal soaring of birds. *American Science*, **50**, 180–209, 1962.

[16] Cone, C.D., A mathematical analysis of the dynamic soaring flight of the albatross. *Virginia Institute of Marine Science*, *Special Scientific Report*, **50**, pp. 1–104, 1964.

[17] Cone, C.D., The aerodynamics of flapping bird flight. *Virginia Institute of Marine Science*, *Special Scientific Report*, **52**, 1968.

[18] Pennycuick, C.J., Power requirements for horizontal flight in the pigeon. *Journal of Experimental Biology*, **49**, pp. 527–555, 1968.

[19] Pennycuick, C.J., A wind-tunnel study of the gliding flight in the pigeon *Columba livia.* *Journal of Experimental Biology*, **49**, pp. 509–526, 1968.

[20] Pennycuick, C.J. The mechanics of bird migration. *Ibis*, **111**, pp. 526–556, 1969.

[21] Pennycuick, C.J., Mechanics of flight. *Avian Biology*, Vol. 5, eds. D.S. Farner & J.R. King, Academic Press: London, New York, pp. 1–75, 1975.

[22] Tucker, V.A., The energetics of bird flight. *Scientific American*, **220**, pp. 70–78, 1969.
[23] Weis-Fogh, T., Energetics of hovering flight in hummingbirds and in *Drosophila. Journal of Experimental Biology*, **56**, pp. 79–104, 1972.
[24] Weis-Fogh, T., Quick estimates of flight fitness in hovering animals, including novel mechanisms for lift production. *Journal of Experimental Biology*, **59**, pp. 169–230, 1973.
[25] Norberg, U.M., Aerodynamics of hovering flight in the long-eared bat *Plecotus auritus. Journal of Experimental Biology*, **65**, pp. 459–470, 1976.
[26] Norberg, U.M., Some advanced flight manoeuvres of bats. *Journal of Experimental Biology*, **64**, pp. 489–495, 1976.
[27] Rayner, J.M.V., A new approach to animal flight mechanics. *Journal of Experimental Biology*, **80**, pp. 17–54, 1979.
[28] Rayner, J.M.V., A vortex theory of animal flight. Part 1. The vortex wake of a hovering animal. *Journal of Fluid Mechanics*, **91**, pp. 697–730, 1979.
[29] Rayner, J.M.V., A vortex theory of animal flight. Part 2. The forward flight of birds. *Journal of Fluid Mechanics*, **91**, 731–763, 1979.
[30] Ellington, C.P., Vortices and hovering flight. *Instationäre Effekte an schwingenden Tierflügeln*, ed. W. Nachtigall, Steiner: Wiesbaden, pp. 64–101, 1980.
[31] Ellington, C.P., The aerodynamics of hovering insect flight. I–IV. *Philosophical Transactions of the Royal Society of London B*, **305**, pp. 1–181, 1984.
[32] Brodsky, A.K., *The Evolution of Insect Flight*, Oxford University Press: New York, 1994.
[33] Pennycuick, C.J., *Bird Flight Performance*, Oxford University Press: Oxford, 1989.
[34] Norberg, U.M., *Vertebrate Flight: Mechanics, Physiology, Morphology, Ecology and Evolution*, Zoophysiol. Series 27, Springer-Verlag: Berlin, Heidelberg, New York, 1990.
[35] Norberg, U.M., Energetics of flight. *Avian Energetics and Nutritional Ecology*, ed. C. Carey, Chapman and Hall: New York, pp. 199–249, 1996.
[36] Rayner, J.M.V., Estimating power curves of flying vertebrates. *Journal of Experimental Biology*, **202**, pp. 3449–3461, 1999.
[37] Alerstam, T., *Bird Migration*, Cambridge University Press: Cambridge, 1990.
[38] Alerstam, T., Bird migration performance on the basis of flight mechanics and trigonometry. *Biomechanics in Animal Behaviour*, eds. P. Domenici & R.W. Blake, Bios: Oxford, pp.105–124, 2000.
[39] Azuma, A., *The Biokinetics of Flying and Swimming*, Springer-Verlag: Tokyo, 1992.
[40] Spedding, G.R., The aerodynamics of flight. *Mechanics of Animal Locomotion*, ed. R.McN. Alexander, Advances in Comparative & Environmental Physiology 11, Springer-Verlag: Berlin, Heidelberg, pp. 51–111, 1992.
[41] Shyy, W., Berg, M. & Ljungqvist, D., Flapping and flexible wings for biological and micro air vehicles. *Progress in Aerospace Science*, **35**, 455–506, 1999.
[42] Hertel, H., *Structure-Form-Movement*, Reinhold: New York, 1966.
[43] Triantafyllou, M.S., Triantafyllou, G.S. & Gopalakrishnan, R., Wake mechanics for thrust generation in oscillating foils. *Physics of Fluids A*, **3**, pp. 2835–2837, 1991.
[44] Anderson, J.M., Streitlien, K., Barrett, D. & Triantafyllou, M.S., Oscillating foils of high propulsive efficiency. *Journal of Fluid Mechanics*, **360**, pp. 41–72, 1998.
[45] Wang, Z.J., Vortex shedding and frequency selection in flapping flight. *Journal of Fluid Mechanics*, **410**, pp. 323–341, 2000.
[46] Nudds, R.L., Taylor, G.K. & Thomas, A.L.R., Tuning of Strouhal number for high propulsive efficiency accurately predicts how wingbeat frequency and stroke amplitude

relate and scale with size and flight speed in birds. *Proceedings of the Royal Society of London B*, **271**, pp. 2071–2076, 2004.

[47] Anderson, J., *Fundamentals of Aerodynamics*, 2nd edn, McGraw-Hill Inc.: Singapore, 1991.

[48] Hummel, D. & Möllenstädt, W., On the calculation of the aerodynamic forces acting on a house sparrow (*Passer domesticus* L.) during downstroke by means of aerodynamic theory. *Fortschritte der Zoologie*, **24**, pp. 235–256, 1977.

[49] Pennycuick, C.J., Gliding flight of the dog-faced bat *Rousettus aegyptiacus* observed in a wind-tunnel. *Journal of Experimental Biology*, **55**, pp. 833–845, 1971.

[50] Tucker, V.A. & Heine, C., Aerodynamics of gliding flight in a Harris' hawk, *Parabuteo unicinctus. Journal of Experimental Biology*, **149**, pp. 469–489, 1990.

[51] Nachtigall, W. & Kempf, B., Vergleichende Untersuchungen zur flugbiologischen Funktion de Daumenfittichs (*Alula spuria*) bei Vögeln. I. Der Daumenfittich als Hochtriebserzeuger. *Zeitschrift für Vergeichende Physiologie*, **71**, pp. 326–341, 1971.

[52] Nachtigall, W., Bird flight: kinematics of wing movements and aspects on aerodynamics. *Proceedings of the 17th International Ornithological Congress*, **1**, pp. 377–383, 1980.

[53] Ellington, C.P., van der Berg, C., Willmott, A.P. & Thomas, A.L.R., Leading-edge vortices in insect flight. *Nature*, **384**, pp. 626–630, 1996.

[54] Dickinson, M.H., Lehmann, F.-O. & Sane, S.P., Wing rotation and the aerodynamic basis of insect flight. *Science*, **284**, pp. 1954–1960, 1999.

[55] Srygley, R.B. & Thomas, A.L.R., Unconventional lift-generating mechanisms in free-flying butterflies. *Nature*, **420**, pp. 660–664, 2002.

[56] Videler, J.J., Stamhuis, E.J. & Povel, G.D.E., Leading-edge vortex lifts swifts. *Science*, **306**, pp. 1060–1962, 2004.

[57] Phlips, P.J., East, R.A. & Pratt, N.H., An unsteady lifting line theory of flapping wings with application to the forward flight of birds. *Journal of Fluid Mechanics*, **112**, pp. 97–125, 1981.

[58] Tucker, V.A., Body drag, feather drag and interference drag of the mounting strut in a peregrine falcon *Falco peregrinus. Journal of Experimental Biology*, **149**, pp. 449–468, 1990.

[59] Pennycuick, C.J., Klaassen, M., Kvist, A. & Lindström, Å., Wingbeat frequency and the body drag anomaly: wind-tunnel observations on a thrush nightingale (*Lucinia lucinia*) and a teal (*Anas crecca*). *Journal of Experimental Biology*, **199**, pp. 2757–2765, 1996.

[60] Hedenström, A. & Liechti, F., Field estimates of body drag coefficient on the basis of dives in passerine birds. *Journal of Experimental Biology*, **204**, pp. 1167–1175, 2001.

[61] Pennycuick, C.J., Obrecht, H.H. & Fuller, M.R., Empirical estimates of body drag of large waterfowl and raptors. *Journal of Experimental Biology*, **135**, pp. 253–264, 1988.

[62] Hedenström, A. & Rosén, M., Body frontal area in passerine birds. *Journal of Avian Biology*, **34**, pp. 159–162, 2003.

[63] Thomas, A.L.R., On the aerodynamics of birds' tails. *Philosophical Transactions of the Royal Society London B*, **340**, pp. 361–380, 1993.

[64] Tucker, V.A., Bird metabolism during flight: evaluation of a theory. *Journal of Experimental Biology*, **58**, pp. 689–709, 1973.

[65] Hedenström, A., Migration by soaring or flapping flight in birds: the relative importance of flight cost and speed. *Philosophical Transactions of the Royal Society London B*, **342**, pp. 353–361, 1993.

[66] Norberg, U.M., Flying, gliding, and soaring. *Functional Vertebrate Morphology*, eds. M. Hildebrand, D.M. Bramble, K.F. Liem & D.B. Wake, Harvard University Press: Cambridge, MA, pp. 129–158, refs. pp. 391–392, 1985.
[67] Pennycuick, C.J., Soaring behaviour and performance of some East African birds, observed from a motor-glider. *Ibis*, **114**, pp. 178–218, 1972.
[68] Lindhe Norberg, U.M., Brooke, A.P. & Trewhella, W.J., Soaring and non-soaring bats of the family Pteropodidae (flying foxes, *Pteropus* spp.): wing morphology and flight performance. *Journal of Experimental Biology*, **203**, pp. 651–664, 2000.
[69] Spedding, G.R., The wake of a kestrel (*Falco tinnunculuc*) in gliding flight. *Journal of Experimental Biology*, **127**, pp. 45–57, 1987.
[70] Katz, J. & Plotkin, A., *Low-Speed Aerodynamics*, Cambridge University Press: Cambridge, 1991.
[71] Norberg, R.Å. & Norberg, U.M., Take-off, landing, and flight speed during fishing flights of *Gavia stellata* (Pont.). *Ornis Scandinavica*, **2**, pp. 55–67, 1971.
[72] Rayleigh, Lord, The soaring of birds. *Nature, London*, **27**, pp. 534–535, 1883.
[73] Pennycuick, C.J. Gust soaring as a basis for the flight of petrels and albatrosses (Procellariiformes). *Avian Science*, **2**, pp. 1–12, 2002.
[74] Scorer, R.S., *Natural Aerodynamics*, Murray: London, 1958.
[75] Pennycuick, C.J., Thermal soaring compared in three dissimilar tropical bird species, *Fregata magnificens, Pelecanus occidentalis,* and *Coragyps atratus. Journal of Experimental Biology*, **102**, pp. 307–325, 1983.
[76] Thollesson, M. & Norberg, U.M., Moments of inertia of bat wings and body. *Journal of Experimental Biology*, **158**, pp. 19–35, 1991.
[77] Pennycuick, C.J., Flight of seabirds. *Seabirds: Feeding Ecology and Role in Marin Ecosystems*, ed. J.P. Croxall, Cambridge University Press: Cambridge, pp. 43–62, 1987.
[78] Herzog, K., *Anatomie und Flugbiologie der Vögel*, Fischer: Stuttgart, 1968.
[79] Norberg, U.M., Hovering flight of the pied flycatcher (*Ficedula hypoleuca*). *Swimming and Flying in Nature*, Vol. 2, eds. T.Y.-T. Wu, C.J. Brokaw & C. Brennen, Plenum Press: New York, pp. 869–881, 1975.
[80] Norberg, U.M., Hovering flight of *Plecotus auritus* Linnaeus. *Bijdragen tot de Dierkunde*, **40**, pp. 62–66, 1970.
[81] Brown, R.H.J., The flight of birds. *Biol. Rev.*, **38**, pp. 460–489, 1963.
[82] Aldridge, H.D.J.N., Body accelerations during the wingbeat in six bat species: function of the upstroke in thrust generation. *Journal of Experimental Biology*, **130**, pp. 275–293, 1987.
[83] Tobalske, B.W. & Dial, K.P., Effects of body size on take-off flight performance in the Phasianidae (Aves). *Journal of Experimen*tal *Biology*, **203**, pp. 3319–3332, 2000.
[84] Spedding, G.R., Rayner, J.M.V. & Pennycuick, C.J., Momentum and energy in the wake of a pigeon (*Columba livia*) in slow flight. *Journal of Experimental Biology*, **111**, pp. 81–102, 1984.
[85] Ellington, C.P., The aerodynamics of normal hovering: three approaches. *Comparative Physiology: Water, Ions, and Fluid Dynamics*, eds. K. Schmidt-Nielsen, L. Bolis & S.H.P. Maddrell, Cambridge University Press: Cambridge, pp. 327–345, 1978.
[86] Norberg, U.M., Kunz, T.H., Steffensen, J.F., Winter, Y. & von Helversen, O., The cost of hovering and forward flight in a nectar-feeding bat, *Glossophaga soricina*, estimated from aerodynamic theory. *Journal of Experimental Biology*, **182**, pp. 207–227, 1993.

[87] Pennycuick, C.J. & Lock, A., Elastic energy storage in primary feather shafts. *Journal of Experimental Biology*, **64**, pp. 677–689, 1976.
[88] Osborne, M.F.M., Aerodynamics of flapping flight with application to insects. *Journal of Experimental Biology*, **28**, pp. 221–245, 1951.
[89] Kirkpatrick, S.J., The moment of inertia of bird wings. *Journal of Experimental Biology*, **151**, pp. 489–494, 1990.
[90] Lindhe Norberg, U.M., Bird flight. *Acta Zoologica Sinica*, **50**, pp. 921–935, 2004.
[91] Lighthill, M.J., Introduction to the scaling of aerial locomotion. *Scale Effects in Animal Locomotion*, ed. T.J. Pedley, Academic Press: New York, pp. 365–404, 1977.
[92] Rayner, J.M.V., The intermittent flight of birds. *Scale Effects in Animal Locomotion*, ed. T.J. Pedley, Academic Press: New York, pp. 37–55, 1977.
[93] Rayner, J.M.V., Bounding and undulating flight in birds. *Journal of Theoretical Biology*, **117**, pp. 47–77, 1985.
[94] Csicsáky, M.J., Body-gliding in the zebra-finch. *Fortschritte der Zoologi*e, **24**, pp. 275–286, 1977.
[95] Norberg, R.Å., Why foraging birds in trees should climb and hop upwards rather than downwards. *Ibis*, **123**, pp. 281–288, 1981.
[96] Norberg, R.Å., Optimum locomotion modes for birds foraging in trees. *Ibis*, **123**, pp. 172–180, 1983.
[97] Norberg, U.M., Evolution of vertebrate flight: an aerodynamic model for the transition from gliding to flapping flight. *American Naturalist*, **126**, pp. 303–327, 1985.
[98] Norberg, U.M., Evolution of flight in birds: aerodynamic, mechanical and ecological aspects. *The Beginnings of Birds*, eds. M.K. Hecht, J.H. Ostrom, G. Viohl & P. Wellnhofer. *Proc. of the Int. Archaeopteryx Conf.*, Eichstätt, 1984, Freunde des Jura-Museums Eichstätt, Willibaldsburg, pp. 293–302, 1985.
[99] Betz, A., Applied airfoil theory. *Aerodynamic Theory*, Vol. 4, ed. W.F. Durand, Dover: New York, pp. 1–129, 1963.
[100] Mises, R. von, *Theory of Flight*, Dover: New York, 1959 (first published 1945).
[101] Houghton, E.L. & Brock, A.E., *Aerodynamics for Engineering Students*, 2nd edn, Arnold: New York, 1960.
[102] Withers, P.C. & Timko, P.L., The significance of ground effect to the aerodynamic cost of flight and energetics of the black skimmer (*Rhynchops nigra*). *Journal of Experimental Biology*, **70**, pp. 13–26, 1977.
[103] Lissaman, P.B.S. & Schollenberger, C.A., Formation flight of birds. *Science*, **168**, pp. 1003–1005, 1970.
[104] Higdon, J.J.L. & Corrsin, S. Induced drag of a bird flock. *American Naturalist*, **112**, pp. 727–744, 1978.
[105] Heppner, F.H., Avian flight formation. *Bird-Banding*, **45**, pp. 160–169, 1974.
[106] Greenewalt, C.H., Dimensional relationships for flying animals. *Smithsonian Miscellaneous Collection*, **144**, pp. 1–46, 1962.
[107] Greenewalt, C.H., The flight of birds. *Transactions of the American Philosophical Society*, **65**, pp. 1–67, 1975.
[108] Rayner, J.M.V., Form and function in avian flight. *Current Ornithology*, ed. R.F. Johnston, Plenum Press: New York, pp. 1–66, 1988.
[109] Tennekes, H., *The Simple Science of Flight: From Insects to Jumbo Jets*, MIT Press: Cambridge, MA, 1996.

[110] Pennycuick, C.J., Mechanical constraints on the evolution of flight. *The Origin of Birds and the Evolution of Flight*, ed. K. Padian, California Academy of Sciences: San Francisco, pp. 83–98, 1986.
[111] Norberg, U.M., Ecological determinants of bat wing shape and echolocation call structure with implications for some fossil bats. *European Bat Research*, eds. V. Hanák, I. Hoprácèk & J. Gaisler, Charles University Press: Praha, pp. 197–211, 1989.
[112] Brower, J.C. & Veinus, J., Allometry in pterosaurs. *University of Kansas Paleontological Contributions Papers*, **105**, pp. 1–32, 1981.
[113] Rayner, J.M.V., Flight adaptations in vertebrates. *Vertebrate Locomotion*, ed. M.H. Day, Symposia of the Zoological Society of London, Academic Press: London, New York, pp. 137–172, 1981.
[114] Rayner, J.M.V., Form and function in avian flight. *Acta XX Congr. Int. Ornithol. (Suppl.)*, New Zealand Ornithological Trust Board: Wellington, p. 265, 1990.
[115] Hill, A.V., The dimensions of animals and their muscle dynamics. *Science Progress in London*, **38**, pp. 209–230, 1950.
[116] Pennycuick, C.J., Wingbeat frequency of birds in steady cruising flight: new data and improved predictions. *Journal of Experimental Biology*, **199**, pp. 1613–1618, 1996.
[117] Taylor, G.K., Nudds, R.L. & Thomas, A.L.R., Flying and swimming animals cruise at a Strouhal number tuned for high power efficiency. *Nature*, **425**, pp. 707–711, 2003.
[118] Ellington, C.P., Limitations on animal flight performance. *Journal of Experimental Biology*, **160**, pp. 71–91, 1991.
[119] Marden, J., From damselflies to pterosaurs: how burst and sustainable flight performance scale with size. *American Journal of Physiology*, **266**, pp. R1077–R1084, 1994.
[120] Tobalske, B.W. & Dial, K.P., Effects of body size on take-off flight performance in the Phasianidae (Aves). *Journal of Experimental Biology*, **203**: 3319–3332, 2000.
[121] Askew, G.N., Marsh, R. & Ellington, C.P., The mechanical power output of the flight muscles of the blue-breasted quail (*Coturnix xhinensis*) during take-off. *Journal of Experimental Biology*, **204**, pp. 3601–3619, 2001.
[122] Pennycuick, C.J., Flight of seabirds. *Seabirds: Feeding Ecology and Role in Marine Ecosystems*, ed. J.P. Croxall, Cambridge University Press: Cambridge, pp. 43–62, 1987.
[123] Andersson, M. & Norberg, R.Å., Evolution of reversed sexual dimorphism and role partitioning among predatory birds, with a size scaling of flight performance. *Biology Journal of Linnaean Society*, **15**, pp. 105–130, 1981.
[124] Norberg, U.M., Morphology of the wings, legs and tail in three coniferous forest tits, the goldcrest, and the treecreeper in relation to locomotor pattern and feeding station selection. *Philosophical Transactions of the Royal Society London B*, **287**, pp. 131–165, 1979.
[125] Norberg, U.M., Flight, morphology and the ecological niche in some birds and bats. *Vertebrate Locomotion*, ed. M.H. Day, Symposia of the Zoological Society of London, Academic Press: London, New York, pp. 173–197, 1981.
[126] Norberg, U.M., Wing design and migratory flight. *Israel Journal of Zoology*, **41**, pp. 297–305, 1995.
[127] Norberg, U.M. & Norberg, R.Å., Ecomorphology of flight and tree-trunk climbing in birds. *Acta XIX Congressus Internationalis Ornithologici*, **2**, pp. 2271–2282, 1989.
[128] Lindhe Norberg, U.M., Structure, form, and function of flight in engineering and the living world. *Journal of Morphology*, **252**, pp. 52–81, 2002.

[129] Dam, C.P., van, Nikfetrat, K. & Vijgen, P.M.H.W., Lift and drag calculations for wings and tails: techniques and applications. *Contemporary Mathematics*, **141**, pp. 463–477, 1993.
[130] Prandtl, L., *Ergebnisse der Aerodynamischen Versuchsanstalt zu Göttingen*, II, Lieferung: München, 1923.
[131] Oehme, H., On the aerodynamics of separated primaries in the avian wing. *Scale Effects in Animal Locomotion*, ed. T.J. Pedley, Academic Press: London, New York, pp. 479–494, 1977.
[132] Hofton, A., How sails can save fuel in the air. *New Science*, **20**, pp. 146–147, 1978.
[133] Hummel, D. The aerodynamic characteristics of slotted wing-tips in soaring birds. *Proceedings of the 17th International Ornithological Congress*, **1**, pp. 391–396, 1980.
[134] Tucker, V.A., Gliding birds: reduction of induced drag by wing tip slots between primary feathers. *Journal of Experimental Biology*, **180**, pp. 285–310, 1993.
[135] Tucker, V.A., Drag reduction by wing tip slots in a gliding Harris' hawk, *Parabuteo unicinctus*. *Journal of Experimental Biology*, **198**, pp. 775–781, 1994.
[136] Andersson, M., *Sexual Selection*, Princeton University Press: Princeton, 1994.
[137] Tucker, V.A., Pitching equilibrium, wing span and tail span in a gliding Harris' Hawk, *Parabuteo unicinctus*. *Journal of Experimental Biology*, **165**, pp. 21–43, 1992.
[138] Norberg, R.Å., Swallow tail streamer is a mechanical device for self-deflection of tail leading edge, enhancing aerodynamic efficiency and flight manoeuvrability. *Proceedings of the Royal Society of London B*, **257**, pp. 227–233, 1994.
[139] Thomas, A.L.R. & Balmford, A., How natural selection shape birds' tails. *American Naturalist*, **146**, 848–868, 1995.
[140] Evans, M.R., Rosén, M., Park, K.J. & Hedenström, A., How do birds' tails work? Delta-wing theory fails to predict tail shape during flight. *Proceedings of the Royal Society of London B*, **269**, pp. 1053–1057.
[141] Pennycuick, C.J., Span-ratio analysis used to estimate effective lift:drag ratio in the double-crested cormorant, *Phalacrocorax auritus*, from field observations. *Journal of Experimental Biology*, **142**, 1–15, 1989.
[142] Thomas, A.L.R., The flight of birds that have wings and a tail: variable geometry expands the envelope of flight performance. *Journal of Theoretical Biology*, **183**, pp. 237–245, 1996.
[143] Rosén, M. & Hedenström, A., Gliding flight in a jackdaw: a wind tunnel study. *Journal of Experimental Biology*, **204**, pp. 1153–1166, 2001.
[144] Spedding, G.R., On the significance of unsteady effects in the aerodynamic performance of flying animals. *Fluid Dynamics in Biology*, eds. A.Y. Cheer & C.P. van Dam, *Contemporary Mathematics*, Vol. 141, American Mathematical Society: Providence, pp. 401–419, 1993.
[145] Rayner, J.M.V., Flight mechanics and constraints on flight performance. *Israel Journal of Zoology*, **41**, pp. 321–342, 1995.
[146] Kuethe, A.M., Prototypes in nature. The carry-over into technology. *TechniUM*, Spring, pp. 3–20, 1975.
[147] Abbott, J.H. & Doenhoff, A.E., *Theory of Wing Sections*, McGraw-Hill in Aeron. Sci.: New York, 1949.
[148] Norberg, U.M., Bat wing structures important for aerodynamics and rigidity. *Zeitschrift für Morphologie der Tiere*, **73**, pp. 45–62, 1972.